UNIVERSITY OF CALGARY

Analysis of a Deterministic Entangled Photon Pair Source using Single Photons

by

Abhirup Goswami

A THESIS

SUBMITTED TO THE FACULTY OF GRADUATE STUDIES

IN PARTIAL FULFILLMENT OF THE REQUIREMENTS FOR THE

DEGREE OF MASTER OF SCIENCE

GRADUATE PROGRAM IN PHYSICS AND ASTRONOMY

CALGARY, ALBERTA

SEPTEMBER, 2016

Abstract

Quantum repeaters are the most promising approach for distributing entanglement over long distances. Recent approaches to develop quantum repeaters involve the use of deterministic entangled photon pair sources. On the other hand heralded entangled photon pair sources have been proposed independently both with parametric down conversion source and single photon sources. We modify the latter scheme to implement it as an on demand entangled photon pair source and analyse its performance considering inefficient detectors, inefficient quantum memories and inefficient single photon sources. We conclude that with the current state of art, generation of high fidelity deterministic entangled photon pairs is possible with moderate efficiency. We then compare the results to the deterministic entangled photon pair source obtainable using parametric down conversion source and conclude that the single photon scheme described in this thesis is more practical for such an implementation.

Acknowledgements

My deepest gratitude to my supervisor Dr. Christoph Simon for his guidance, counsel and encouragement throughout my study and research. This thesis would not have been possible without his immense support and understanding during the entire course of my masters in University of Calgary.

I would like to thank Dr. Nicolas Sangouard and Dr. Hugues De Riedmatten for their valuable ideas. I express my appreciation to Dr. Simon Trudel, Dr. Wolfgang Tittel and Dr. Paul Barclay for having served on my committee. I deeply value their thoughtful questions, comments and reviews.

My thanks to the members of the Department of Physics and Astronomy and my fellow graduate students for their co-operation and help.

I am deeply indebted to Dr. Raedler, Dr. Baird, Ms. Jan Crook for their immense support through out the duration of my degree.

A big thanks to my entire family and my friends Robyn, Aveek, Rahul, Esha, Michael for their continuous love and encouragement.

And finally to Pupu, without whom, I probably would not have been writing this.

Table of Contents

List of Figures and Illustrations

Chapter 1

Introduction

The discovery of entanglement [1] has led to the most extensive research in quantum physics in recent years. Mathematically speaking entangled states are those quantum states of compound systems which cannot be written as product states of individual subsystems [2].For example we can imagine a spin singlet state shared between two observers A (Alice) and B (Bob) who are separated by a distance.

$$\left|\Psi^{-}\right\rangle = \frac{1}{\sqrt{2}}(\left|\uparrow\right\rangle_A \left|\downarrow\right\rangle_B - \left|\downarrow\right\rangle_A \left|\uparrow\right\rangle_B)) \tag{1.1}$$

where the qubit of subsystem belonging to Alice is represented by $(\left|\uparrow\right\rangle_A, \left|\downarrow\right\rangle_A)$ and the qubit of subsystem belonging to Bob is represented by $(\left|\uparrow\right\rangle_B, \left|\downarrow\right\rangle_B)$. The spin is measured in z direction for each of the subsystems.

Clearly such a joint state cannot be written as product of states shared by Alice and Bob individually. Let us also imagine that Alice chooses to measure the spin of her subsystem in z direction and let Bob know her choice via classical communication. The curious feature of entanglement is that if Bob also chooses to measure the spin of his subsystem in z direction , then the result obtained by him is always anti-correlated with that of Alice's result. If Alice has obtained spin up for her subsystem then Bob will end up finding his spin down for his subsystem. And if Alice has obtained spin down for her subsystem, then Bob will end up finding spin up for his subsystem. It is, as if, Bob's spin had no well defined spin initially, but the measurement made by Alice, albeit at a distant location, has somehow influenced Bob's spin to be anti correlated. This directly challenges our pre conception (locality, realism) [1] of classical physics.

An initial explanation [3] to this problem was to state that quantum mechanics is an incomplete theory and one needs additional classical parameters, namely the local variables, to explain it. However, one can ask, what if Bob is not obedient to the choice of the basis made by Alice and

measures in any direction other than z? How will the correlations of the result look like in that case? In the historic paper [1], John Bell deduced that if local variable theories are true, such disobedience from Bob's part would ensure that all correlation functions resulting out of joint measurements between Alice and Bob, can vary only within a specific range of values. This result is famously known as the Bell inequality [1].

One of the most interesting feature of entanglement is that for an entangled state, once can perform joint measurements where the value of the correlation function thus obtained, violates Bell inequality or its analogous form [2]. Violation of Bell inequalities have been experimentally confirmed through numerous experiments [4], [5]. Recently, a loophole free Bell test [6] has been reported.

In quantum information processing, entanglement has led to pioneering ideas such as quantum teleportation [7], quantum dense coding [8] and quantum key distribution [9] thus leading to quantum internet [10].

In the Ekert protocol [9] of the quantum key distribution, in the presence of an eavesdropper Eve, Alice wants to transfer a secret key to Bob in a secured way. This key thus shared can be subsequently used to exchange publicly encrypted message between Alice and Bob. However Alice might not always succeed as Eve can intercept the key midway and perform a measurement to decipher it. But measurement alters a quantum system. So Eve's measurement will alter the original key and thus Bob will not receive the original key Alice intended to send. So the question is, how will Bob, upon reception of the key from Alice, know whether Eve has successfully intercepted it or not? Here Alice and Bob shares strings of Bell states on which they can perform local measurements (from a certain choice of basis). Alice now informs Bob her measurement results for each basis via classical communication. And Bob compares her results with his own and computes a correlation function. Ekert protocol formulates that, had Eve failed to intercept their message, then this correlation function will violate Bell inequality. If the initial photons shared are maximally entangled, then this correlation function will violate Bell inequality maximally. However, if the correlation function fails to violate accordingly, then Bob can know that Eve has succeeded in

eavesdropping.

It is a well known result in quantum communication that transferring one qubit can only transfer at most one bit of classical information [11]. However, quantum dense coding [8] exhibits that it is possible to send two bits of classical information via transferring one qubit if the qubit is entangled in a Bell state with another qubit at the receivers end. Bell states is a maximally entangled states of two qubits. There are four possible Bell states and they are

$$\left|\Psi^{-}\right\rangle = \frac{1}{\sqrt{2}}(\left|0\right\rangle_A \left|1\right\rangle_B + e^{i\pi} \left|1\right\rangle_A \left|0\right\rangle_B)) \tag{1.2}$$

$$\left|\Psi^{+}\right\rangle = \frac{1}{\sqrt{2}}(\left|0\right\rangle_A \left|1\right\rangle_B + e^{i2\pi} \left|1\right\rangle_A \left|0\right\rangle_B)) \tag{1.3}$$

$$\left|\Phi^{-}\right\rangle = \frac{1}{\sqrt{2}}(\left|0\right\rangle_A \left|0\right\rangle_B + e^{i\pi} \left|1\right\rangle_A \left|1\right\rangle_B)) \tag{1.4}$$

$$\left|\Phi^{+}\right\rangle = \frac{1}{\sqrt{2}}(\left|0\right\rangle_A \left|0\right\rangle_B + e^{i2\pi} \left|1\right\rangle_A \left|1\right\rangle_B)) \tag{1.5}$$

An interesting property of Bell state is that if any one of them is chosen by Alice and Bob, either Alice or Bob can perform a local unitary rotation on it to obtain the other Bell states. There are four such possible rotations (I, σ_x,$-i\sigma_y$, σ_z) and thus we can encode two bits for each of them. For example we can say $00 \equiv I$, $01 \equiv \sigma_x$,$10 \equiv -i\sigma_y$,$11 \equiv \sigma_z$. In quantum dense coding, Alice and Bob lying at two distant location, share a Bell state which they know beforehand. Now Alice can perform any of the four rotations mentioned above on her qubit, and send her qubit to Bob. Now Bob can perform joint measurement on Alice's qubit and his qubit to infer which rotation was exactly performed by Alice. As each such rotation encodes two bits, in this way Alice can send Bob two bits of information by only sending one qubit.

Also if Alice and Bob shares a Bell state, which is initially known, Alice can transfer an unknown qubit to Bob without physically transporting it. This is the method of quantum teleportation [7]. In this case, Alice couples the qubit to be sent with the Bell state previously shared between her and

Bob. She can then perform a local Bell state measurement on her initial qubit (which is entangled with Bob's qubit) and the qubit to be sent. This Bell state measurement entangles the two qubit in Alice's hand into any of the four possible Bell state but collapses Bob's qubit to a product state. If Alice can now inform Bob classically which Bell state her measurement has inferred, Bob will be able to perform local unitary operation on his qubit to retrieve the original Alice intended to send. The common feature of all these examples of applications of quantum information processing, is that we need entangled states shared between distant locations. Photons travel faster than any other known medium and that they interact weakly with the environment. This makes entangled photon states the primary choice for sharing entanglement over distance. However the main problem in this approach is that direct transmission of photons over long distance is difficult as they get absorbed by optical fibres and for distances around $600km$ the rate of transmission falls to very low values [12] .

One of the principal way to solve this problem is using quantum repeaters as proposed by Briegel et al[13]. The well known implementation of quantum repeaters by Duan, Lukin, Cirac and Zoller, DLCZ protocol[14] has triggered wide range of experimental interests. One of the recent and more practical approaches to repeaters [15] (to be discussed in details next chapter) uses deterministic entangled photon pair sources.

Photon source(s) coupled with linear optics elements and photon detectors are capable of producing entangled photon pairs [16], [17] where such creation is signalled by appropriate detections in the detectors, thus being heralded. This entangled photon state can be subsequently stored in quantum memories to be recalled upon. This leads one to ask whether we can have deterministic entangled photon pair sources fabricated in this way. In this thesis we propose a scheme which can be ideally implemented as deterministic entangled photon pair sources. This scheme uses single photon sources, quantum memories, photon number resolving detectors and linear optic elements and is inspired from [17]. We calculate its performance under practical imperfections and deduce under what range of imperfections can it function as deterministic entangled photon sources.

Heralded entangled photon pairs, which is the basic idea behind our scheme, can also be implemented using parametric down conversion sources [16]. Inspired from this, we imagine another scheme which can possibly be implemented as deterministic entangled photon sources. We compare these two schemes and draw conclusions for future.

1.0.1 Arrangement of the thesis

The rest of the thesis follows in the following way-

In Chapter 2 *Background* we briefly discuss the relevance of our thesis in the frame work of current research in quantum information processing. We briefly discuss quantum repeaters and a more recent repeater scheme involving entangled photon pair sources thus the latter's importance. In Chapter 3 *Ideal Scheme*, we propose our scheme as a deterministic entangled photon pair source and state the condition under which it can act so. In chapter 4 *Imperfect Scheme* we then introduce our imperfections considered and inspect the sensitivity of the scheme to the imperfections. In chapter 5 *Performance as a deterministic source*, we discuss its feasibility both under practical imperfections and realistic improvements in technology. We also compare it with another possible scheme which is shown in *Appendix 2*. In *Discussions*, we discuss the summary of our results. Outline of calculations for the scheme discussed in this thesis have been shown in *Appendix 1*.

Chapter 2

Background

This chapter describes the relevance of this thesis in current research in quantum information processing. In this chapter we follow a quantum repeater protocol and importance of deterministic entangled photon pair sources in the frame work of this repeater scheme

2.1 Quantum Repeaters

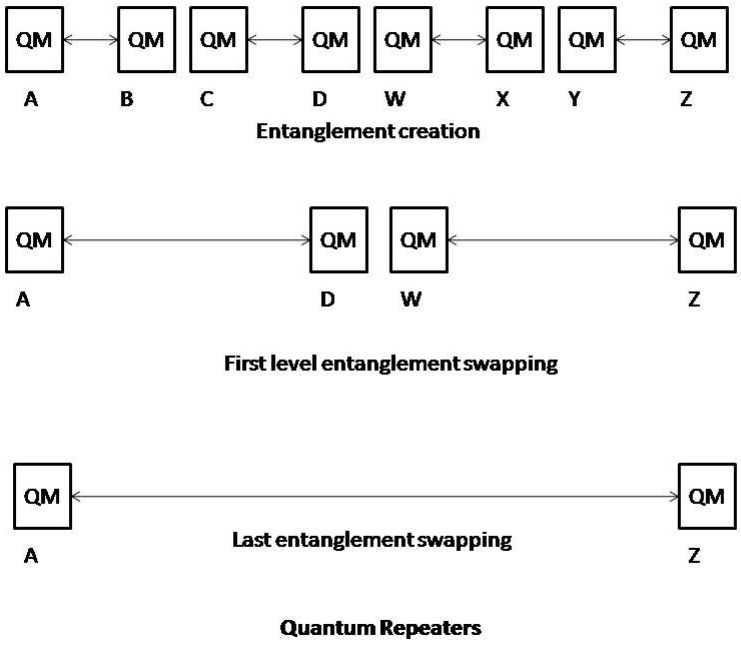

Figure 2.1: Basic scheme for quantum repeaters as proposed by Briegel et al [13]

When it comes down to sharing entangled photon states, the obvious choice would have been to create entanglement locally and then transmit one subsystem to a distant location. But as photon absorption increases exponentially with the length of the fibre, even with the best available re-

sources, this makes the rate of transmission fall to very low values for distances around 600 km [18],[12]. A solution to this problem was proposed by Briegel et al [13] under the name quantum repeaters (figure (2.1)).

Here, say we want entanglement to be shared between two distant locations A and B separated by a distance L. This distance L is divided into n elementary links each of distance $L_0 = L/n$. Each elementary link is equipped with one node at each of its ends. Entanglement is generated independently in the elementary link and is subsequently stored in the nodes . Once entanglement is established in neighbouring links, entanglement swapping [19](see section A.7) is performed between elementary links, and subsequently on secondary and tertiary links till the final entangled state shared between A and B. Quantum memories [20] are the principal choice for these nodes. The idea behind using quantum memories (chapter 2, section 2) is to ensure that entanglement can be generated independently along each elementary link and stored till the next link is ready for swapping.

The DLCZ protocol uses three level atomic ensembles as its nodes. These atomic ensembles emit a single photon via spontaneous Raman Transition while creating a single atomic excitation. Ideally both the ensembles are excited, and any of one of them emit a photon with equal probability, which then travels to a central station. Its detection heralds the other single atomic excitation de localised among the two atomic ensembles, thus generating the entanglement over the elementary link. This de localised atomic excitation can be read out with a strong resonant light pulse to emit anti-stokes photons to perform entanglement swapping via one photon detection (see section A.7). They are then combined into a beam splitter followed by detectors at each end. An alternative approach [21] is to using a combination quantum memories and photon pair source has also been proposed aiming better performance.

2.2 Quantum memories

Quantum memories [20],[22] are important elements for quantum information processing applications such as quantum networks [10], quantum repeaters [13],[15] and linear optical quantum computation [23].

Quantum memories for single photons can be thought of a black box which intakes a single photon state and re emits another single photon state. Its performance can be evaluated by two important parameters- firstly, the probability that it re emits a single photon given the absorption of a single photon. This probability is termed as the *efficiency*. Secondly the overlap of the emitted state of the photon with the absorbed state, which is called the *conditional fidelity*. For an ideal quantum memory both efficiency and conditional fidelity takes the value of unity. In addition to these, important parameters that characterizes a quantum memory are - the *bandwidth* of a quantum memory, which is the range of frequency in which it can function; the *storage time*, which is defined as the time for which it can store the absorbed photon and subsequently recalled. This time of recall can either be fixed by the system or ”on demand” thus chosen by the user. Also the wavelength range of the re emitted photons is important in certain cases where the outgoing photon is transmitted via optical fibre.

Single photon quantum memories relies on light matter coupling through various media such as nitrogen vacancy centres in diamond [25],[26],[27],[28],[29], optically trapped atoms [30], Raman scattering in solids [31],[32] and alkali vapours have been observed [33], [34],[35] and rare earth ion doped solids. Principal approaches in fabricating quantum memories with rare earth ion doped solids involve controlled and irreversible broadening (CRIB)[36], [37], [38], [39], [40], [41] and atomic frequency comb (AFC) [42], [43], [44], [45], [46], [47], [48], [49], [15]

2.3 A recent repeater protocol

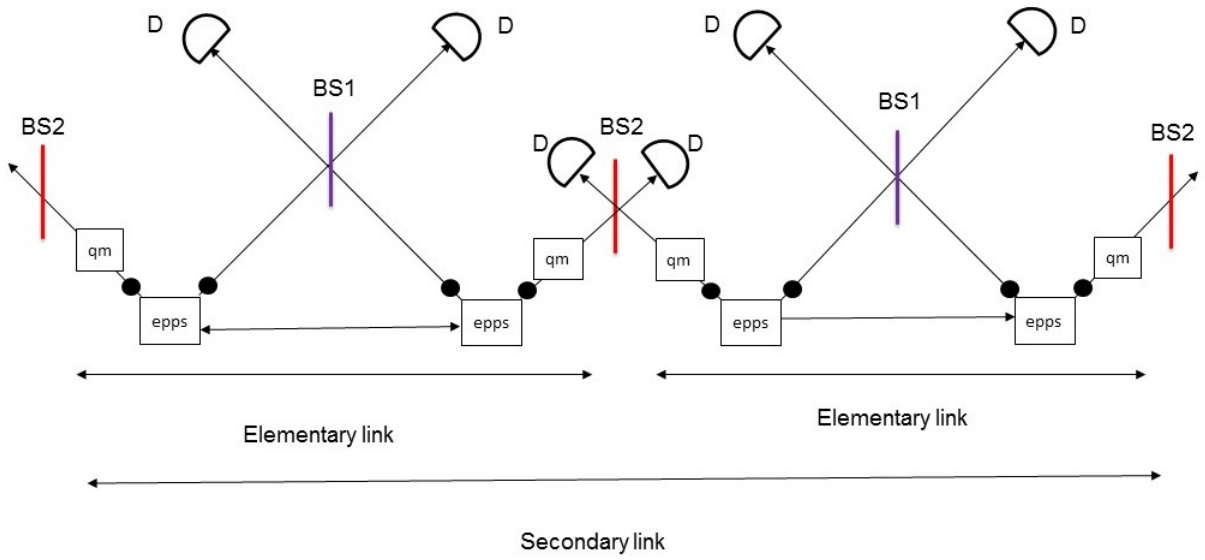

Figure 2.2: Simplified version of a more recent approach to quantum repeaters [15]. Here photon pair sources which ideally emits entangled photon pairs are marked as epps. BS1 and BS2 refers to 50 : 50 beam splitters. A 50 : 50 beam splitter can transmit or reflect a photon with equal probability. Quantum memories are marked as qm and photon number resolving detectors are marked as D

We here, in figure 2.2, focus on the simplified (non multiplexed) version of a more recent approach [15] where they have outlined quantum repeater architecture with pair sources and quantum memories. A source generating entangled photon pair (epps) lies at each end of an elementary link. Each such source emits a pair of entangled photons one of which is stored in the quantum memory and the other is transmitted over a quantum channel to a central station where it meets the similar member generated from the pair sources in the other end of the link. At the central station, the joint state of two such photons undergoes a Bell state measurement with a beam splitter ($BS1$) and two single photon detectors aiming for joint detection of photons, one in each detector. This result is communicated via a classical channel to herald entanglement among the photons stored in the respective quantum memories. This entanglement is stored within the quantum memories till the same heralding occurs for adjacent links. Then, for entanglement swapping [19] via two

photon detection (see section A.7) photons are recalled from the quantum memories and similar Bell state measurement is performed at beam splitter ($BS2$). With classical communication this heralds entanglement within adjacent links. This procedure is repeated till entanglement over the final distance is achieved.

It is possible to implement this repeater scheme *with multiplexing*. In multiplexing, the source emits a train of photon pairs in distinct optical modes instead of a single pair. One photon from each pair reaches the central station while the other is stored in the quantum memory. The large number of photons increases the probability of detection at the central station thus increasing the entanglement generation rate over the elementary link. Entanglement swapping requires recombination of the same photon modes whose partners heralds the entanglement. And although the number of photon pairs permissible is limited by the storage capacity of the quantum memory, the overall entanglement distribution time achievable is significantly lower than for other protocols [18].

In temporal multiplexing photon pairs with the same frequency arrive at different time to the central station. An individual pair from the sources are distinguished according to the time taken by them to reach the detector. Thus in order to ensure retrieval of their corresponding partner one needs the quantum memory to have a variable recall time time. Rare earth ion doped crystals at cryogenic temperature have been demonstrated as promising photon storage devices for temporal multiplexing [44],[45],[46],[47],[48].

The original proposition [15] also proposes use of spectral multiplexing [49], [15]. Unlike temporal multiplexing, in spectral multiplexing the train of photons arrive at the same time but they have different frequencies. In this case, one does not need the quantum memories to have different storage time but one uses a frequency shifter to retrieve an output photon with the desired frequency. However it also required that the beam splitters used in the central station are capable of distinguishing photons based on their frequencies. It has been shown that allowing standard imperfections, this protocol outperforms direct transmission [50] for practical distances. The same

paper [15] has also demonstrated efficient highly broadband quantum memories capable of storing upto 26 spectral modes using high frequency. In future, one can envisage combining the ideas of temporal, spectral and spatial multiplexing [51] to achieve a high number of modes [52],[45] which promises practical implementation of quantum repeaters.

2.4 Photon pair sources

2.4.1 Parametric Down Conversion

Photon pair sources are important in the implementation of the repeater scheme discussed in the previous section. If a pump laser is incident on non linear crystals such as beta barium borate or potassium dihydrogen phosphate, a pair of entangled photons can emerge with a certain probability. This process is known as parametric down conversion and it is the most practical source of entangled photons available [53]. In this regard, it is obvious to ask whether it is possible to use them as photon pair sources in this protocol.

If a PDC source emits a pair of photon with probability p, then the probability of two such sources (one at each end)each emitting a pair is p^2. However it is also possible that one such source emits two pairs with a probability proportional to p^2 while the other source fails to emit any. This an unwanted case. Thus the error varies in the same order as that of the desired case. This is the principal problem of using PDC as a pair photon source. For a more practical implementation, we look for deterministic photon pair source, where probability of multi pair emission is much lower than that of the square of the probability of single pair generation. This leads us to using deterministic entangled photon pair sources.

2.4.2 Deterministic entangled photon pair sources

A deterministic single photon source ideally emits a pair of entangled photons at the convenience of the experimenter. It is desired that it emits a pair with a high probability, denoted as efficiency

E of the source, as this efficiency contributes to the overall entanglement distribution rate of the repeater protocol. It is also desired that the pair thus emitted has a high overlap with desired entangled state as this would enhance the fidelity of the final entanglement shared between A and B. We denote this probability as the conditional fidelity f of the source. One can note that the values of E and f can be optimized in order to enhance the secret key distribution rate [50], [54] for the repeater protocol.

2.4.3 Quantum dots as photon pair sources

The principal approach in fabricating deterministic entangled photon pair source has been made by using quantum dots.

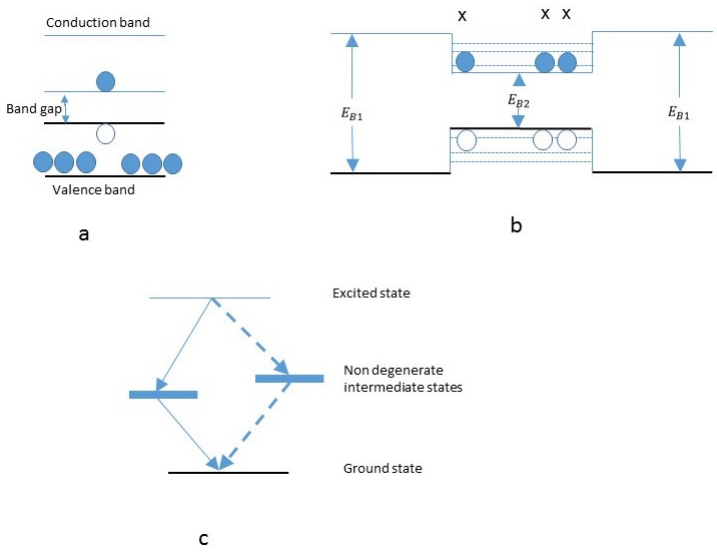

Figure 2.3: Schematic diagram of quantum dots as single photon sources.a) The valence band of a semiconductor is filled with electrons one of which can be excited to the conduction band leaving a hole behind. The energy difference between the valence and the conduction band is called the band gap. b) A semi conductor with a lower band gap can be embedded inside another semi conductor with a higher band gap thus creating a finite potential well. An electron (X) trapped in the finite potential well can spontaneously recombine with the hole it has left behind to emit a photon. A spin singlet state (XX) trapped in the finite potential well can spontaneously recombine with the hole pair it has left behind to emit pair of polarization entangled photons. c) Once one of the electron of the singlet pair has recombined with the hole, the remaining one can recombine with its hole via one of two non degenerate intermediate state

A semiconductor is composed of a lower energy band, initially filled with electrons, and a higher energy conduction band separated by an energy difference called the band gap. One or more electrons can be excited from the valence band to the conduction band leaving a hole behind (figure 2.3 a). Now if we have two such semiconductors of different band gap $(E_{B1}, E_{B2}, E_{B1} > E_{B2})$, we can embed the one with the smaller band gap E_{B2} within the one with the higher band gap E_{B1} to form a finite potential well (figure 2.3 b).

Now if an electron in the valence band in the embedded semiconductor is excited to its conduction band X with an energy E_B, $(E_{B2} < E_B < E_{B1})$, it will be trapped in the finite potential well leaving a hole behind. This electron can now spontaneously recombine with the hole to emit a single photon. If the excitation energy $E_B > E_{B1}$, then the excited photon will initially not be trapped within the finite potential well, but it can lose energy via interaction with phonons to fall back in to the well. Single photon sources using quantum dots using Purcell enhanced quantum dot micro-pillar system has been experimentally achieved [55].

If instead of a single photon, a spin singlet state of electron (XX) is excited to the conduction band, it can recombine with the pair of holes to emit a pair of polarization entangled photons[56]. Here the emission of the first photon brings a the system into the manifold of intermediate single excitation states (figure 2.3 c). Had these intermediate excitation states been degenerate, the emitted photon would have been perfectly entangled. However these states are naturally not degenerate. Thus the path chosen by the second photon is not ambiguous. This makes the outgoing photon pair mostly classically co-related rather than entangled. This is a major hindrance in producing entangled photon pairs using quantum dots. The degree of entanglement can be increased to a measurable level by spectrally filtering out most of the un-entangled photon pair [57], but this introduces photon loss. Recent approach [58] has succeeded producing entangled photon pairs using nano-wires with embedded quantum dots. Their single photon extraction efficiency $\sim 18\%$ which makes the two photon extraction efficiency have a low value $\sim 3\%$. Finding an alternative approach to deterministic entangled photon sources with higher efficiency is our principal motivation.

2.5 A short note of single photon sources

2.5.1 Single Photon Sources

Single photon sources [59] are important in linear optical quantum computing. Ideally a single photon source should satisfy four conditions.

• It should be on demand. This means that the experimenter can choose when the photon is emitted.

• It should be able to emit indistinguishable photons.In particular this means the emitted photons have identical wave packets in time or in frequency domain.

• The rate of generation of single photon is arbitrarily fast, only limited by the pulse duration.

• And finally source should emit a single photon with unit probability thus the probability of multi pair being zero.

Apart from this, an important characteristic of a single photon source is the wavelength at which the photon is emitted.

A single photon source is parametrized by its efficiency ε, which is defined as the fraction of triggers that leads to a single photon emission in the output modes. However, for an imperfect single photon source, multiple emission occurs. This feature is parametrized by the second order correlation function $g^{(2)}$[59].

second order correlation function

This definition comes from the experimental model of the Hanbury Brown and Twiss interferometer. In this model, a light beam is divided among two detectors by a non-polarizing beam splitter and the correlation of the detections is observed. The formal definition of the second order correlation function is given by

$$g^{(2)}(\tau) = \frac{\left\langle a^{\dagger}(t+\tau)a^{\dagger}(t)a(t+\tau)a(t)\right\rangle}{\left\langle a^{\dagger}(t)a(t)\right\rangle^{2}} \tag{2.1}$$

where $a^{\dagger}$ is the creation operator for the incoming mode.

For a classical light, which exhibits a bunching effect $g^{(2)}(0) \geq 1$. For example, in a chaotic ther-

mal state of light, $g^{(2)}(\tau) = g^{(2)}(0) = 2$, which is its upper limit. However, for a coherent state produced by the laser, which can be both understood in terms of semi classical and quantum formalism, the emitted photons are independent of each other which gives $g^{(2)}(\tau) = g^{(2)}(0) = 1$.
For a fock state $|n\rangle$ we have $g^{(2)}(0) = 1 - \frac{1}{n}$ which gives us $g^{(2)}(0) = 0$ for an ideal single photon state. Further excitations of the single photon source are supposed to emit more photons which introduces a new condition $g^{(2)}(\tau) > g^{(2)}(0)$ for such sources.

In this thesis the calculation starts on an incoming state (equation A.9)

$$|\psi\rangle_j = [\sqrt{(1-\varepsilon_1)}e^{i\theta'_{0j}}I + \sqrt{\varepsilon_1(1-\varepsilon_2)}e^{i\theta'_{1j}}a_j^\dagger + \sqrt{\frac{\varepsilon_1\varepsilon_2}{2}}e^{i\theta'_{2j}}a_j^{\dagger 2}]|0\rangle \tag{2.2}$$

For this state if we calculate the expression of $g^{(2)}(0)$ we have

$$g^{(2)}(0) = \frac{2\varepsilon_2}{\varepsilon_1(1+\varepsilon_2)^2} \tag{2.3}$$

In this thesis we have only assumed first order error in ε_2 (see equation A.3)
There we have

$$\varepsilon_2 = \frac{g^{(2)}(0)\varepsilon_1}{2 - 2g^{(2)}(0)\varepsilon_1} \approx \frac{g^{(2)}(0)\varepsilon_1}{2} \tag{2.4}$$

2.5.2 SPS with PDC and memories

A spontaneous parametric down conversion when coupled with quantum memories can serve as a single photon source. One photon from the source is detected by a single photon detector while the other photon enters the quantum memory. Successful single photon detection heralds the memory charging. This stored photon is retrieved on demand (within the storage time of the quantum memory). If the conditional fidelity of the quantum memory is high then we are assured that the retrieved state is the desired state and high memory efficiency reduces the possibility of vacuum emission approximating it to an ideal single photon source.

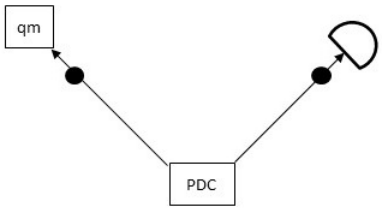

Figure 2.4: Scheme showing use of quantum memories as single photon sources:- Pair photons are emitted from the pair source. One of the emitted photon charges the quantum memory which is heralded by the detection of the second photon.

As the PDC source emits a pair of photon, detection of a single photon in the detector will herald its counterpart in the quantum memory.

Now a single turn of illumination of a perfectly heralded PDC emits a single pair with probability p but it also emits higher other pairs with other probabilities (equation B.7) such as two pairs with probability with $\frac{3}{4}p^2$, and so on. Considering up to two pair emissions, given a single detection in the heralding detector, the probability that a photon is actually heralded is p_{eff} where

$$p_{eff} = \frac{p\eta_d + 2 \times \frac{3}{4}p^2\eta_d(1-\eta_d)}{1+p+\frac{3}{4}p^2} \tag{2.5}$$

In our scheme we have four sources. In case we have a photon heralded in a quantum memory for one source, we have to wait for the other three quantum memories (acting as single photon sources in other three cases) to get charged. This will continue till the four sources are charged. This introduces a waiting time factor T_f in our scheme. If the repetition rate of the PDC source is R_{PDC} and the waiting time factor for charging of the four memories is T_f then the total time T_{tot} of four such detections at four single photon sources as

$$T_{tot} = T_f(\frac{1}{R_{PDC}})(\frac{1}{p_{eff}})$$

Thus giving us the effective repetition/heralding rate R_{rep}

$$R_S = \frac{1}{T_f}R_{PDC}p_{eff} \tag{2.6}$$

If we wait for time T_w for the first source, then the average waiting time for the second source is $\frac{T}{2}$, for the third source it is $\frac{T}{3}$ and for the fourth source it is $\frac{T}{4}$. This makes the estimated value of T_f

as $\frac{25}{12}$.

We come back to the original scenario where we have perfectly heralded PDC emits a pair of photons and detection of one of them in a detector heralds its counterpart in the quantum memory. We only consider the case where there is one such detection and we allow only the error case where two photons have been emitted by the pair and one of them have been missed by the detector. If we ignore photon losses before it reaches the memory, the photon state reaching the detector, assuming error linear in p, can be written as

$$\rho = \frac{1}{p_1^2 + p_2^2}(p_1^2 \left|1\right\rangle \left\langle 1\right| + p_2^2 \left|2\right\rangle \left\langle 2\right|)$$

As this state is heralded by a single detection in the detector, we have with $p_1^2 = 1, p_2^2 = \frac{3}{2}p(1-\eta_d)$ Now if the memory efficiency is η_m and we write the input state in the pure state formalism, we have

$$\left|\Phi\right\rangle = (p_1 e^{i\theta_1''} a + p_2 e^{i\theta_2''} \frac{1}{\sqrt{2}} a^2) \left|0\right\rangle$$

Following the beam splitter model of loss (Appendix A, section 6), we now introduce the following loss transformations

$$a^\dagger = \sqrt{\eta_m} a_{em}^\dagger + \sqrt{1-\eta_m} a_l^\dagger$$

where a_{em} and a_l are emitted and lost modes respectively. Then in the final form of density matrix we have

$$\rho = \frac{1}{p_1^2 + p_2^2}((p_1^2(1-\eta_m) + p_2^2(1-\eta_m)^2) \left|0\right\rangle \left\langle 0\right| + (p_1^2\eta_m + 2p_2^2\eta_m(1-\eta_m)) \left|1\right\rangle \left\langle 1\right| + p_2^2\eta_m^2 \left|2\right\rangle \left\langle 2\right|)$$

We compare this with the density matrix of the input state we use in this thesis

$$\rho = (1-\varepsilon_1) \left|0\right\rangle \left\langle 0\right| + \varepsilon_1(1-\varepsilon_2) \left|1\right\rangle \left\langle 1\right| + \varepsilon_1\varepsilon_2 \left|2\right\rangle \left\langle 2\right|$$

and from there we can write we have

$$\varepsilon_1 = \frac{2 + 3p(1-\eta_d)\eta_m(2-\eta_m)}{2 + 3p(1-\eta_d)} \tag{2.7}$$

and

$$\varepsilon_2 = \frac{3}{2}\frac{p\eta_m(1-\eta_d)}{(1+\frac{3}{2}p(1-\eta_d)(1-\eta_m))} \tag{2.8}$$

Chapter 3

Ideal scheme

In this chapter we discuss the principal topic of this thesis, implementing deterministic entangled photon pair source based on single photon sources and quantum memories

3.1 Description of the scheme

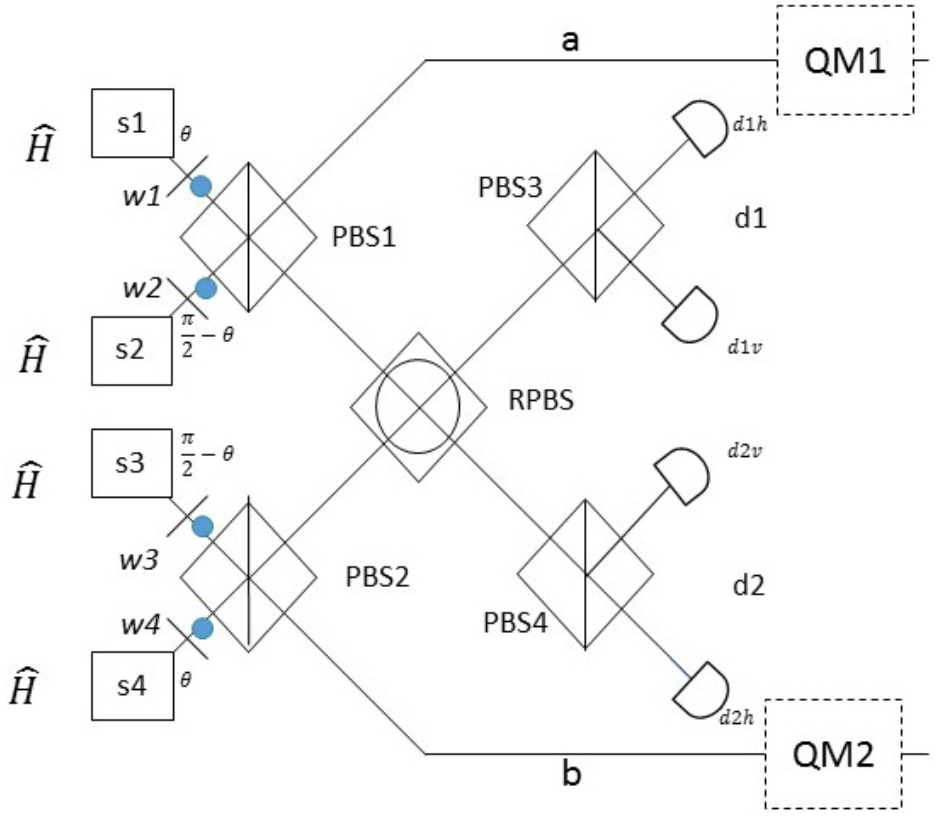

Figure 3.1: Deterministic entangled photon pair source using sing photon pair sources

There are four independent but identical single photon sources, marked $s1$, $s2$, $s3$, $s4$ in the diagram. Ideally, each of them simultaneously emit four indistinguishable single photons, all of them

polarized in the horizontal mode. Each photon passes through a half wave plate marked $w1$, $w2$, $w3$, $w4$ in the diagram. The angle of rotation for $w1$ and $w4$ is θ. The respective angles for $w2$ and $w3$ are $\frac{\pi}{2} - \theta$. Thus they are complementary angles. Photons from $s1$ and $s2$ interfere at polarizing beam splitter $PBS1$ and photons from $s3$ and $s4$ interfere at polarizing beam splitter $PBS2$. One output from each of these polarizing beam splitters make the output modes a and b, which end up in a pair of identical quantum memories, marked $QM1$ and $QM2$. The role of these quantum memories is to store the outgoing photons which are then recalled at a time decided by the experimenter. The other two output modes, one from $PBS1$ and one from $PBS2$ meet at a third rotated polarizing beam splitter, rotated in the $\frac{\pi}{4}$ basis, marked $RPBS$. The output modes from this $RPBS$ are incident on two other polarizing beam splitters, marked $PBS3$ and $PBS4$ respectively. Two output modes from $PBS3$ end up in two photon number resolving detectors marked $d1h$ and $d1v$. Two output modes from $PBS4$ end up in two photon number resolving detectors marked $d2h$ and $d2v$. Ideally if we have a joint detection in such a way that one detection occurs at any one of the detector set $(d1h, d1v)$ and another detection occurs at any one of the detector set $(d2h, d2v)$, then we have a Bell state heralded in the output mode.

This scheme is inspired from the one mentioned by Zhang et al [17] except that in the original scheme, a polarization rotator with $\theta = \frac{\pi}{4}$ has been used for all the four sources where in this scheme θ is a free parameter. The reason for this modification is explained in chapter 4, section 4.2. Also the two quantum memories $QM1$ and $QM2$ have been introduced here in order to store the outgoing photons only to be recalled by the experimenter. Thus the quantum memories are used to realize this scheme as a *deterministic* source.

3.2 Heralded entanglement

3.2.1 Choice of detectors

In order to understand how entanglement is heralded in this circuit given the detections as outlined above, we will have a brief look at some interesting properties of the *RPBS* where we have two incident photons and two emerging photons.

A) If two photons are incident on it through any one input, then they will always emerge from the same output, irrespective of whether they emerge in the same or different polarization, as shown in Appendix A section 5.1.

B)If two indistinguishable photons emerge from it each from one output, then they must have entered the *RPBS* through two different input modes as shown in Appendix A section 5.2.

Now if we have joint detection one from each of the detector set $d1h, d1v$ and the detector set $d2h, d2v$ then we know that two photons have emerged one from each output of the *RPBS* and thus from B)they have entered from two input of the *RPBS*. One of the photons entering the *RPBS* must have come either from $s1$ or $s2$ with equal probability while the other has come either from $s3$ or $s4$ with the same probability. This ensures entanglement of the outgoing photons in the output mode. Here the equal probability is ensured by the presence of the half wave plates

Again if we have joint detection in $d1h - d1v$ (or $d2h - d2v$) then we know they must have entered the *RPBS* from the same input. This gives rise to cases where we have two photons in any of the output mode and none in the other. This is not desired as if we aim to apply this source in the quantum repeater architecture, we need two photons, one from each output mode. Thus such detections are ignored.

For the rest of the thesis we will use the terminology *desired joint detection* to signify joint detection one from each detector set $d1h, d1v$ and $d2h, d2v$. We will use the word *undesired joint detection* to signify joint detections both in the same set, i.e. detector combinations $d1h - d1v$ or $d2h - d2v$.

3.2.2 Nature of generated entanglement

From Appendix A section 5.3 we see that

A) If incoming photons (one at each input) have same polarization, i.e. both horizontally polarized or both vertically polarized, with the same probability, then they will emerge with opposite polarization, i.e. one of them horizontally polarized and the other vertically polarized, with the same probability.

B)If they enter with opposite polarization, i.e. one of them horizontally polarized and the other vertically polarized, with the same probability,then they will emerge with same polarization, i.e. both horizontally polarized or both vertically polarized, with the same probability.

Thus if the photons are detected in the detector pair $d1h - d2h$ (or $d1v - d2v$) then one can see that they have emerged from the two output of *RPBS* with the same polarization (from B)). So they must have entered it from two different input but with opposite polarization. This assures that the entangled state heralded in the quantum memories is $|\Psi\rangle$. Where

$$|\Psi\rangle = \frac{1}{\sqrt{2}}(|V_{s1}\rangle\,|H_{s3}\rangle + |H_{s2}\rangle\,|V_{s4}\rangle) \tag{3.1}$$

Similarly if the photons are detected in the detector pair $d1h - d2v$ (or $d1v - d2h$) then one can see that they have emerged from the two output of the *RPBS* with opposite polarization (from A)). So they must have entered it from two different input with same polarization. This assures that the entangled state heralded in the quantum memories is $|\Phi\rangle$. Where

$$|\Phi\rangle = \frac{1}{\sqrt{2}}(|V_{s1}\rangle\,|V_{s4}\rangle + |H_{s2}\rangle\,|H_{s3}\rangle) \tag{3.2}$$

Denoting qubit A as $|0\rangle_A \equiv |V_{s1}\rangle$, $|1\rangle_A \equiv |H_{s2}\rangle$ and qubit B as $|1\rangle_B \equiv |H_{s3}\rangle$, $|0\rangle_B \equiv |V_{s4}\rangle$ we have $|\Phi\rangle \equiv |\Phi^+\rangle$ and $|\Psi\rangle \equiv |\Psi^+\rangle$ where $|\Phi^+\rangle$ and $|\Psi^+\rangle$ are Bell states in standard basis

3.3 As deterministic pair source

The two quantum memories, $QM1$ and $QM2$ in the output modes ensures that the entangled photons in the outgoing modes are stored for time τ_s where τ_s is their storage time. The on demand nature of a scheme implies that a pair of entangled photon is always available for the experimenter whenever he or she chooses to retrieve it from the quantum memories. This implies that the rate of desired joint detection (which ideally heralds entangled photons in the quantum memories) should be greater than τ_s^{-1}. For clarity of our scheme, we impose the condition that this rate must be greater than τ_s^{-1} *at least by an order* . We refer to this as the **deterministic criterion**

3.4 Figures of Merit

3.4.1 Probability of desired detection

p_s signifies the probability that a desired joint detection takes place given the initial photon states are prepared from the source. Mathematically,

$$p_s = 4\frac{tr[\rho_s]}{tr[\rho_{input}]} \tag{3.3}$$

where ρ_s is the density matrix after that desired joint detection and ρ_{input} is the density matrix of the system at input. The factor 4 comes from the fact that there are four combinations of desired joint detection [d1h-d2h, d1h-d2v, d1v-d2h, d1v-d2v] and any one will serve our purpose.
In our calculations, we have normalized the incoming state, so we have

$$p_s = 4tr[\rho_s] \tag{3.4}$$

Ideally,

$$p_s = \frac{1}{8}(\sin 2\theta)^4 \tag{3.5}$$

where θ is the angle of rotation for the half wave plates along the sources $s1$ and $s3$. Thus we can see that ideally, the probability of desired joint detection is maximized for $\theta = \frac{\pi}{4}$ and the maximum probability is $\frac{1}{8}$

3.4.2 Rate of desired detection

R_s signifies the number of desired joint detection per second. Mathematically this is given by

$$R_s = p_s \times R_{rep} \tag{3.6}$$

where R_{rep} is the repetition rate of the source measured in Hz

3.4.3 Scheme Efficiency

E_s signifies the probability of retrieving at least one photon from each of the quantum memories $QM1$ and $QM2$. Mathematically

$$E_s = \frac{tr[\rho_E]}{tr[\rho_s]} \tag{3.7}$$

where ρ_E is the density matrix of the output state where at least one photon is retrieved from the quantum memories.

Ideally $E_s = 1$

3.4.4 Conditional fidelity

Assuming one photon is retrieved from each of the quantum memories, f_s, the conditional fidelity is the overlap of the output state with the desired entangled state. Mathematically

$$f_s = \frac{tr[\rho_{bellstate}\rho_E]}{tr[\rho_E]} \tag{3.8}$$

Ideally $f_s = 1$

Chapter 4

Scheme including imperfections

In this chapter, we introduce the imperfections to the ideal scheme described in the last chapter and understand the performance of this scheme considering detectors with non unit efficiency, memories with non unit efficiency and single photon sources with non unit efficiency and a small probability of multiple emission only considered upto first order. More specifically, we study the variation of scheme efficiency E_s and scheme fidelity f_s with these imperfections. We also look into the role of the angle of polarization and how its variation is significant to the scheme

4.1 Imperfections

The three sources of loss in this scheme are the sources, the detectors and the quantum memories respectively. So far we have assumed the ideal case where they are perfect but that is not true in practical cases. So we introduce some parameters here which will characterize these imperfections. For the detector we introduce η_d, the detector efficiency. η_d denotes the probability that an incoming photon is detected. For the quantum memory we introduce memory efficiency η_m which denotes the probability that given a stored photon is extracted in its original stored state. For the source, we introduce source efficiency ε_1 and the two photon component ε_2. ε_1 denotes the probability that the single photon source emits at least one photon and ε_2 denotes the probability that the single photon source also emits two photons, in a single mode, assuming that it emits at least one photon. It is referred to as the two photon component. In this thesis we limit ourselves to the case where only one of the sources emits two photons.

The literature of single photon sources use the terminology second order correlation function $g^{(2)}$.

Here $\varepsilon_2 \approx \frac{1}{2}g^{(2)}(0)\varepsilon_1$ as mentioned in equation 2.4.

Without imperfections, as pointed out in chapter 3, section 4.3 and section 4.4, scheme efficiency $E_s = 1$ and scheme fidelity $f_s = 1$. However if the detectors, sources and quantum memories are not ideal, a desired joint detection does not necessarily lead to storage of a photon in each quantum memories. For example - one or more sources can misfire or the one or more detectors can fail to detect photons thus leading to false detections. And even if two photons are stored in the memories, their inefficiency might render the photons non retrievable. There are several possibilities of these errors but all lead to the scheme efficiency $E_s \leq 1$ and the conditional fidelity $f_s \leq 1$. To implement this scheme as a deterministic single photon source in the framework of the quantum repeater as mentioned in chapter 2, section 4.2, we desire to maximise scheme efficiency E_s and conditional fidelity f_s (see chapter 2 section 4.2). So it is fairly obvious to say that we need close to perfect detectors, sources and quantum memories to maximize scheme efficiency E_s. But as we do not have a perfect world, the obvious question comes, to what extent the scheme efficiency E_s varies with these imperfections.

4.2 Scheme efficiency

From the expression of scheme efficiency (equation A.58) Here we look at four graphs showing the variation of scheme efficiency E_s with each of the imperfections. In these graphs, experimental values for memory efficiency $\eta_m = 0.69$[60], $\eta_m = 0.87$ [61], $\eta_m = 0.56$ [43], and detector efficiency $\eta_d = 0.88$ [62] are assumed. Wherever required, we assume that the single photon sources have efficiency $\varepsilon_1 = (0.9, 0.75, 0.6)$ and two photon component $\varepsilon_2 = 0.005$.

4.2.1 Graphs

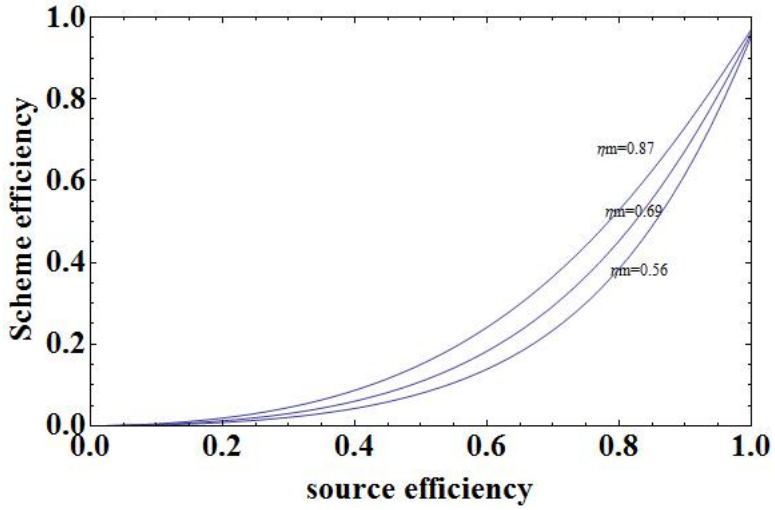

Figure 4.1: Variation of scheme efficiency E_s with source efficiency ε_1 for detector efficiency $\eta_d = 0.88$, memory efficiency $\eta_m = (0.56, 0.69.0.87)$, two photon component $\varepsilon_2 = 0.005$, and $cos^2\theta = 0.1$ where θ is the angle of half wave plate $w1$ (figure 3.1)

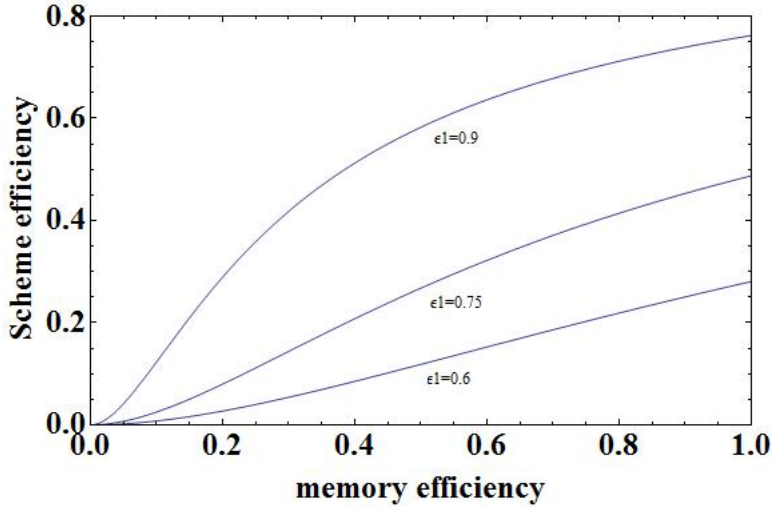

Figure 4.2: Variation of scheme efficiency E_s with memory efficiency η_m for detector efficiency $\eta_d = 0.88$, source efficiency $\varepsilon_1 = (0.6, 0.75.0.9)$, two photon component $\varepsilon_2 = 0.005$, and $cos^2\theta = 0.1$ where θ is the angle of the half wave plate $w1$ (figure 3.1)

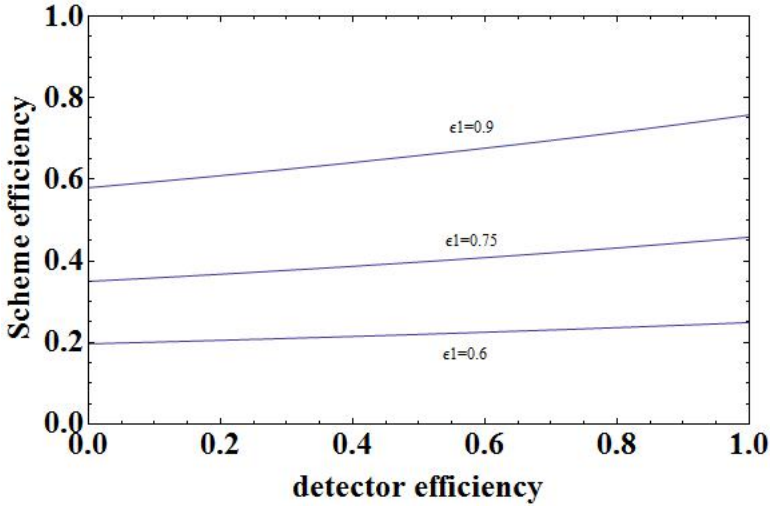

Figure 4.3: Variation of scheme efficiency E_s with detector efficiency η_d for memory efficiency $\eta_m = 0.87$, source efficiency $\varepsilon_1 = (0.6, 0.75.0.9)$, two photon component $\varepsilon_2 = 0.005$, and $cos^2\theta = 0.1$ where θ is the angle of the half wave plate $w1$ (figure 3.1)

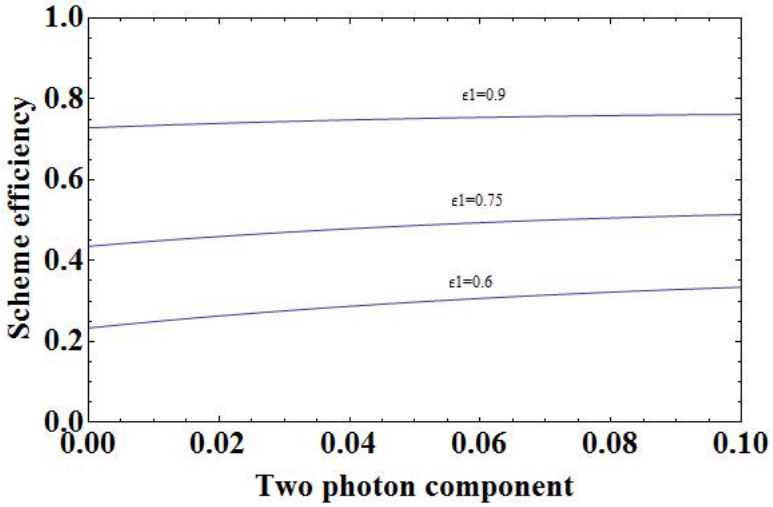

Figure 4.4: Variation of efficiency E_s with two photon component ε_2 for memory efficiency $\eta_m = 0.87$, source efficiency $\varepsilon_1 = (0.6, 0.75, 0.9)$, detector efficiency $\eta_d = 0.88$ and $cos^2\theta = 0.1$ where θ is the angle of the half wave plate $w1$ (figure 3.1)

4.3 Conditional fidelity

From the equation A.62, we see that for small values of ε_2 it is possible to write conditional fidelity f_s as a linear function of ε_2. Thus one can see that a small change in the two photon component ε_2 can cause a significant change in the conditional fidelity f_s. This is exhibited in the following graphs.

4.3.1 Graphs

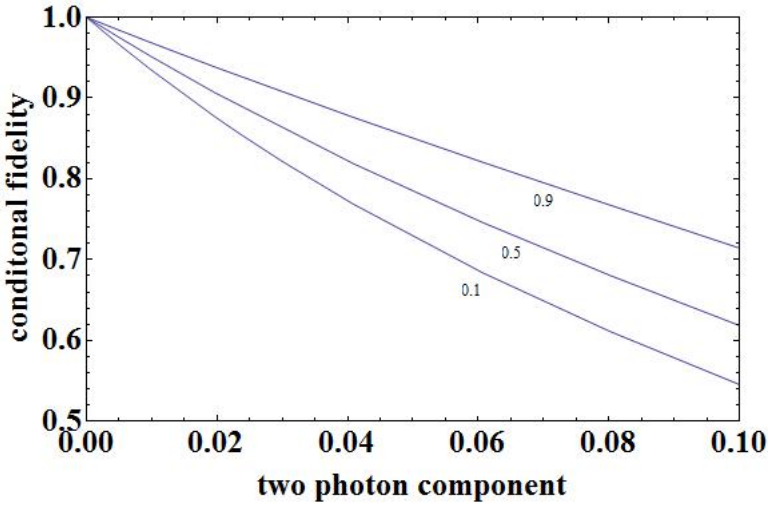

Figure 4.5: Variation of conditional fidelity f_s with two photon component ε_2 for memory efficiency $\eta_m = 0.87$, source efficiency $\varepsilon_1 = 0.9$, detector efficiency $\eta_d = 0.88$ and $cos^2\theta = (0.1, 0.5, 0.9)$ where θ is the the angle of the half wave plate $w1$ (figure 3.1)

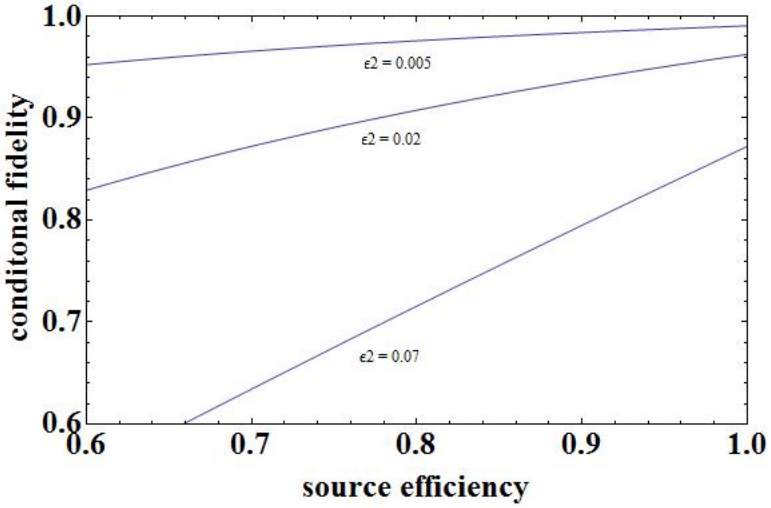

Figure 4.6: Variation of conditional fidelity f_s with source efficiency ε_1 for memory efficiency $\eta_m = 0.87$, two photon component $\varepsilon_2 = 0.005, 0.02, 0.07$, detector efficiency $\eta_d = 0.88$ and $cos^2\theta = 0.9$ where θ is the angle of the half wave plate $w1$ (figure 3.1)

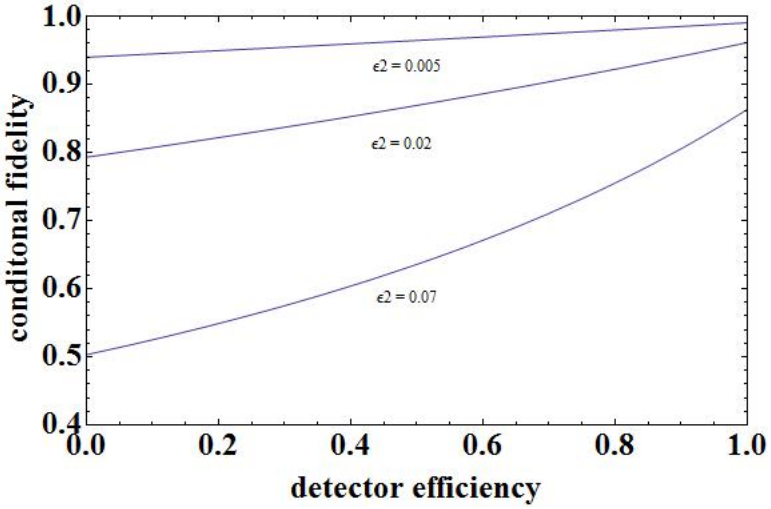

Figure 4.7: Variation of conditional fidelity f_s with detector efficiency η_d for memory efficiency $\eta_m = 0.87$, two photon component $\varepsilon_2 = 0.005, 0.02, 0.07$, source efficiency $\varepsilon_1 = 0.9$ and $cos^2\theta = 0.9$ where θ is the angle of the half wave plate $w1$ (figure 3.1)

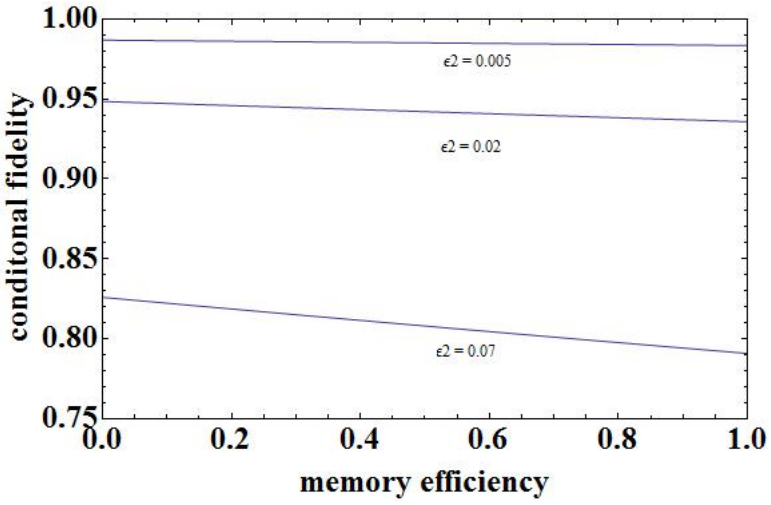

Figure 4.8: Variation of conditional fidelity f_s with memory efficiency η_m for detector efficiency $\eta_d = 0.88$, two photon component $\varepsilon_2 = 0.005, 0.02, 0.07$, source efficiency $\varepsilon_1 = 0.9$ and $cos^2\theta = 0.9$ where θ is the angle of the half wave plate $w1$ (figure 3.1)

4.4 Conclusions

From graph 4.1 we can say that the scheme efficiency E_s is highly affected by the source efficiency ε_1. It is therefore important for us to have high values of ε_1 to make this scheme work in the framework of the repeater protocol as mentioned in chapter 2, section 4.2. From Graph 4.2 and Graph 4.3 we see that for high values of ε_1, scheme efficiency E_s is also sensitive (although to a lesser extent compared to the source efficiency) to the memory efficiency η_m and detector efficiency η_d, and high values of them are desired. However graph 4.4 shows that it is much less sensitive to the two photon component ε_2 as compared to source, memory and detector efficiency. For conditional fidelity however Graph 4.5 shows that unlike scheme efficiency E_s, the conditional fidelity f_s is highly sensitive to the two photon component ε_2 compared to other inefficiencies considered here. This is significant if we want to implement our single photon sources with parametric down conversion and quantum memories as low value of ε_2 implies that the photon pair emission probability p from parametric down conversion source needs to be limited to low values (equation 2.8) but that

would limit the effective repetition rate (equation 2.5 and 2.6).

4.5 Role of the half wave plate

The angle θ of the half wave plate $w1$ (figure 3.1) is not an imperfection but a free parameter chosen in this scheme. As mentioned in chapter 3 section 1, the angle of rotation for half wave plates $w1$ and $w4$ are θ while the angle of rotation of the half wave plates $w2$ and $w3$ is $\frac{\pi}{2} - \theta$ We inspect its role in the following graphs

4.5.1 Graphs

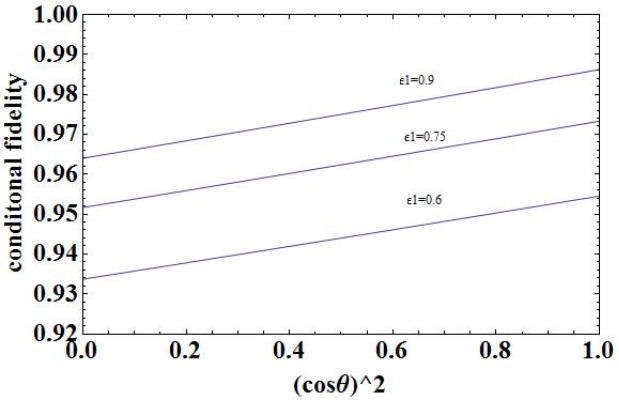

Figure 4.9: Variation of conditional fidelity f_s with $cos^2\theta$ where θ is the the angle of the half wave plate $w1$ (figure 3.1). We assume detector efficiency $\eta_d = 0.88$, two photon component $\varepsilon_2 = 0.005$, memory efficiency $\eta_m = 0.87$ and source efficiency $\varepsilon_1 = (0.6, 0.75, 0.9)$

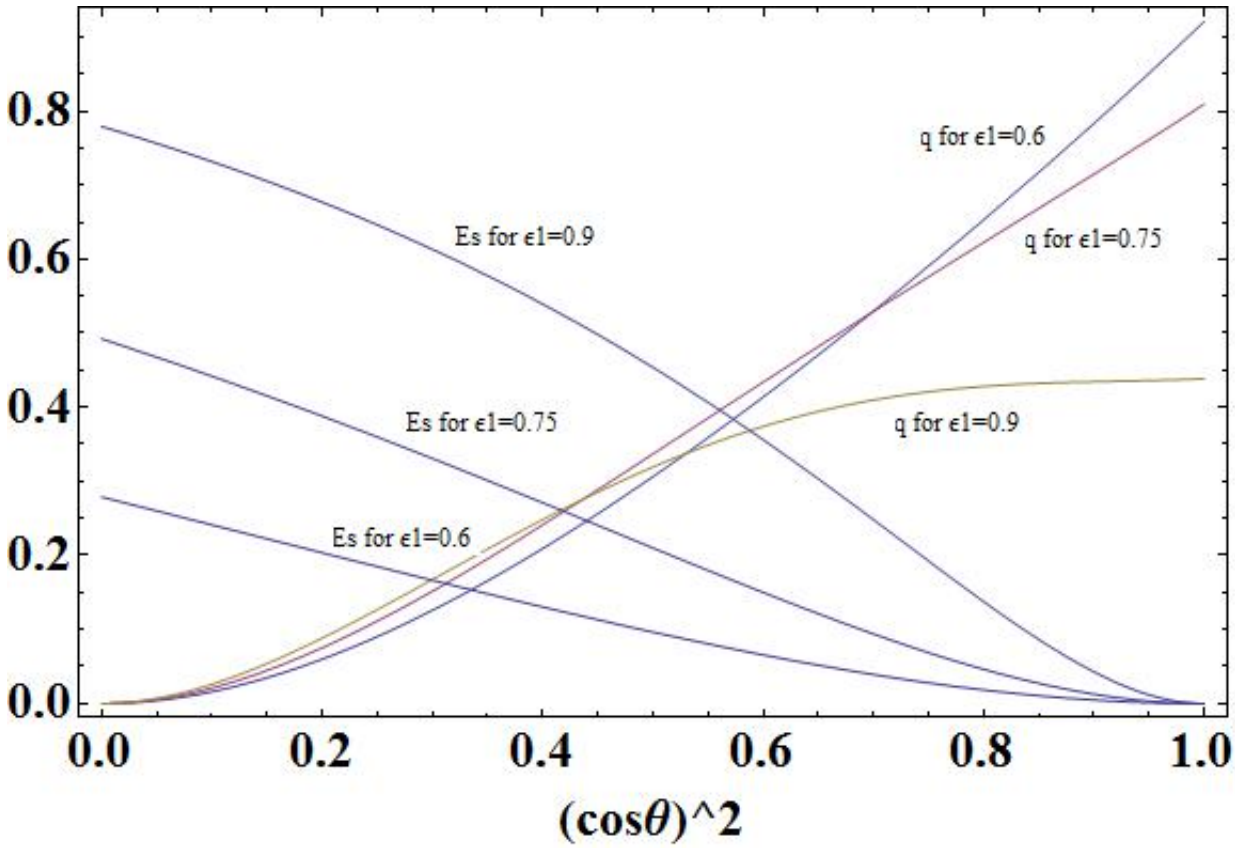

Figure 4.10: Variation of scheme efficiency E and probability of joint detection p_s with $cos^2\theta$ where θ is the angle of the half wave plate $w1$ (figure 3.1). We assume detector efficiency $\eta_d = 0.88$, two photon component $\varepsilon_2 = 0.005$, source efficiency $\varepsilon_1 = 0.9$ and memory efficiency $\eta_m = (0.6, 0.75, 0.9)$. Here $q = 3 \times p_s$ is plotted to ensure visibility.

4.5.2 Conclusions

From graph 4.10 we can see that the scheme efficiency E_s increases sharply with θ while the probability of joint detection p_s decreases sharply with θ. This leads to a significant *trade off* that happens between the rate of desired detection R_s and scheme efficiency E_s.

We recall from chapter 2, section 4.2, that when implemented in the repeater protocol, the scheme efficiency E_s directly influences the entanglement distribution rate of the repeater while the conditional fidelity f_s directly influences the overall fidelity of the repeater protocol. An increment in θ

increases the scheme efficiency E_s and also decreases (although to a lesser extent) the conditional fidelity f_s, as seen from graph 4.9. Thus one can, in principle, choose θ in order to optimize the secret key distribution rate [50] [54] for this repeater protocol.

Chapter 5

Performance as a deterministic source

In this chapter we discuss the feasibility of implementing this scheme as a deterministic entangled photon pair source both under current state of art and under realistic improvement in technology

5.1 Performance as an on demand scheme

5.1.1 Practical regime

The state of art photon number resolving detectors has been reported with efficiency $\eta_d = 0.88$ [62]. Quantum memories with high efficiency such as $\eta_m = 0.69$ using solid state media [60]and $\eta_m = 0.87$ using rubidium vapour [61] have been reported. Both of these memories have a storage time in the order of μs. The repeater protocol we have discussed [15] uses multiplexed AFC memories. The best reported AFC memory [43] has an efficiency $\eta_m = 0.56$ with storage time also in the order of μs. But the authors expect to have much longer time in foreseeable future.

Single photon sources can be implemented using quantum dots. Single photon source [55] have been reported with efficiency $\varepsilon_1 = 0.66$ and a $g^{(2)}(0) = 0.009$, (which leads to $\varepsilon_2 = 0.0029$ from equation 2.4), have been reported. It has a repetition rate in the order of $\sim GHz$

It is also possible to implement single photon sources using parametric down conversion and quantum memories as described in chapter 2 section 5.2. Recall that, for a perfectly heralded PDC source, a detection in the detector heralds the storage of a photon in the quantum memories, which is subsequently retrieved as a single photon. In such an implementation, it is important to limit the pair production probability to a low value in order to avoid higher order emissions. The probability of a pair emission from a PDC is tunable in any experiment. We here have chosen a value 0.047 to give us a range of conditional fidelity f_s which is comparable to the case of quantum dots. Thus,

following equations 2.7 and 2.8, if we implement single photon sources using a perfectly heralded parametric down conversion and quantum memories, using a quantum memory with efficiency $\eta_m = 0.87$ we can obtain $\varepsilon_1 = 0.87$, $\varepsilon_2 = 0.01$, with a quantum memory efficiency $\eta_m = 0.69$ we can obtain $\varepsilon_1 = 0.69$, $\varepsilon_2 = 0.007$, with efficiency $\eta_m = 0.56$ we can obtain $\varepsilon_1 = 0.56$, $\varepsilon_2 = 0.004$. But the rate of repetition in all these cases are $1.5MHz$ (assuming the quantum memory has appropriate bandwidth).

Considering all these practical possibilities, the predicted values have been outlined in the following two tables -

Performance of this scheme as deterministic entangled photon pair sources using quantum dots as single single photon sources at the current state of art.							
Detector efficiency η_d	Memory efficiency η_m	Source efficiency ε_1	Two Photon Component ε_2	Polarizer Angle In degrees θ	Scheme efficiency E_s	Conditional Fidelity f_s	Rate of desired Detection R_s in sec^{-1}
88%	87%	66%	0.29%	45	13%	97.1%	10^8
				60	24%	96.8%	3.3×10^7
				75	32%	96.6%	2.7×10^6

Figure 5.1: For current state of art implementation using quantum dot single photon sources, with source efficiency $\varepsilon_1 = 0.66$ and $\varepsilon_2 = 0.0029$, this table shows theoretically predicted values of efficiency E, conditional fidelity f, rate of desired detection R for different angles of the half wave plate - $45^\circ, 60^\circ, 75^\circ$. Here the detector efficiency $\eta_d = 0.88$, memory efficiency $\eta_m = 0.87$ and repetition rate of the source is $1GHz$

Performance of this scheme as deterministic entangled photon pair sources using PDC and quantum memories as single photon sources at current state of art							
Detector efficiency η_d	Memory efficiency η_m	Source efficiency ε_1	Two Photon Component ε_2	Polarizer Angle In degrees θ	Scheme efficiency E_s	Conditional Fidelity f_s	Rate of desired Detection R_s in sec^{-1}
88%	87%	87%	0.9%	45	39%	96.2%	1.6×10^5
				60	58%	95.4%	6.2×10^4
				75	68.5%	95%	5.8×10^3
	69%	69%	0.7%	45	11.2%	94.3%	1.4×10^5
				60	21.7%	93.8%	4.2×10^4
				75	29.7%	93.4%	3.4×10^3
	56%	56%	0.6%	45	3.8%	93.1%	1.2×10^5
				60	8.1%	92.8%	3.2×10^4
				75	12%	92.6%	2×10^3

Figure 5.2: For current state of art implementation using combination of PDC and quantum memory as single photon sources, this table shows theoretically predicted values of efficiency E, conditional fidelity f, rate of desired detection R for different angles of the half wave plate $45^\circ, 60^\circ, 75^\circ$ respectively. The source efficiency ε_1 and ε_2 is determined from the choice of the quantum memory. Here the detector efficiency $\eta_d = 0.88$, memory efficiency $\eta_m = 0.87$. The parametric down conversion source is assumed to emit a perfectly heralded pair of photons with probability 0.047. It is assumed to have a repetition rate of $100MHZ$ with appropriate memory bandwidth which gives an effective repetition rate for each of the four sources $1.5MHz$

5.1.2 Futurist regime

We can expect research in future to give us better performing components. Keeping that in mind, we predict the performance of this scheme in two particular cases. In the first case, we implement our scheme using quantum dot sources with efficiency 0.9 but assume the current state of art for every other component. In the second case we think about a scenario where all the resources are almost perfect, i.e. the detector, source, and memory efficiency, all equal to 0.96 and the two photon component as low as 0.001. We put forward our predictions in these two cases in the two following table

Performance of this scheme as deterministic entangled photon pair sources using quantum dots as single single photon sources. Current state of art for photon number resolving detectors and quantum memories have been assumed but with optimist efficiency for quantum dot sources							
Detector efficiency η_d	Memory efficiency η_m	Source efficiency ε_1	Two Photon Component ε_2	Polarizer Angle In degrees θ	Efficiency E_s	Conditional Fidelity f_s	Rate of desired Detection R_s in sec^{-1}
88%	87%	90%	0.4%	45	45.3%	97.9%	1×10^8
				60	64.6%	97.5%	4.2×10^7
				75	74.7%	97.2%	4.07×10^6

Figure 5.3: This table shows theoretically predicted values of efficiency E, conditional fidelity f, rate of desired detection R for different angles of the half wave plate $45^\circ, 60^\circ, 75^\circ$ respectively for a quantum dot single photon source with source efficiency $\varepsilon_1 = 0.9$ and $\varepsilon_2 = 0.004$. Current state of art values have been assumed for all other resources. Detector efficiency $\eta_d = 0.88$, memory efficiency $\eta_m = 0.87$

Performance of this scheme as deterministic entangled photon pair sources implementing single photon sources both with using both quantum dots and PDC and quantum memories combination in the futurist regime.				
Polarizer Angle In degrees θ	Efficiency E	Conditional Fidelity f	Rate of desired detection with implementing single photon sources using PDC + Quantum memory combination with R in sec^{-1} The assumed repetition rate is $1.5MHz$	Rate of desired detection with implementing single photon sources using quantum dots R in sec^{-1} The assumed repetition rate is $1\ GHz$
45	76.7%	99.5%	1.7×10^5	1.17×10^8
60	86.4%	99.4%	8×10^4	5.8×10^7
75	90.5%	99.3%	9×10^3	6.2×10^6

Figure 5.4: This table shows theoretically predicted values of efficiency E, conditional fidelity f, rate of desired detection R for different angles of the half wave plate $45°, 60°, 75°$ with source efficiency $\varepsilon_1 = 0.96$ and $\varepsilon_2 = 0.001$, detector efficiency $\eta_d = 0.96$, memory efficiency $\eta_m = 0.96$

5.1.3 Conclusions

Assuming indistinguishable photons emitted from the four single photon sources,from figure 5.1, we can conclude that at the current state of art (photon number resolving detectors with detector efficiency of 88% [62], quantum memories with efficiency 87 % and storage time in μs [61]), one can realize this scheme as an entangled photon pair source if one implements single photon sources using quantum dots (source efficiency $\varepsilon_1 = 0.66$, two photon component $\varepsilon_2 = 0.0029$) [55]. In that case one obtain high conditional fidelity $f_s \sim 97\%$ but with moderate efficiency $E_s \sim 24\%$.
However if one thinks about realizing single photon sources using PDC and quantum memories, this scheme cannot work as an entangled photon pair sources at the current state of art as shown

in figure 5.2. This is because the rate of generation of deterministic entangled photon pair is not sufficiently high. If a PDC source works at $100MHz$, the effective rate comes down below $\sim MHz$ and with current quantum memories of storage time $\sim \mu s$ this does not satisfy our **deterministic criterion** (chapter 3,section 3). A quantum memory of storage time at least $\sim 100\mu s$ is required.

As shown in figure 5.3, we can expect research in quantum dots to advance in future where we can have quantum dot single photon sources with efficiency as high as 90%. Assuming in that case they still have repetition rate of GHz, it is possible to use them as single photon sources to obtain conditional fidelity $\sim 97\%$ and an efficiency $\sim 65\%$.

We can also expect future research to give us quantum memories with storage time more than the current one. If we want to implement single photon sources using PDC and quantum memories, higher storage time of quantum memories will enable the sources to satisfy the **deterministic criterion** (chapter 3,section 3). If the storage time reaches $\sim ms$ even with the current available memory efficiency we can implement a combination of PDC and quantum memories as single photon sources (chapter 2, section 5.3) to implement this scheme as deterministic entangled photon pair sources with efficiency as high as 58% and conditional fidelity 95%.

From figure 5.4, we can say that in the very optimistic regime where we can expect to have photon number resolving detectors having efficiency 96%, and quantum memories to have an efficiency 96% and quantum dot sources with efficiency 96% and acting in GHz regime, we can have almost perfect conditional fidelity and scheme efficiency as high as 86%. If in addition to this, these quantum memories have storage time in *ms*, one can implement the single photon sources using the quantum memories and PDC to attain the same high values of scheme efficiency and conditional fidelity.

5.2 Comparison with another scheme

So far we have seen that the current state does not provide us with resources which can make our scheme work as a deterministic source of entangled photon pair with *high* efficiency. But we can

wait for better resources to appear in future. In that light, we can ask whether this scheme is the only possibility to have such pair sources. The answer, however, is that there is another scheme [16] generating heralded entanglement, which used a parametric down conversion source instead of single photon sources and which can be implemented as a deterministic pair source using quantum memories. This scheme is described in Appendix 2

As we have assumed a perfectly heralded a PDC source (Appendix 2 section 3) for this scheme, to make a comparison on equal footing, we assume a very high source efficiency $\varepsilon_1 = 0.97$ for our scheme. Then we compare the results of these two cases under two circumstances. Firstly, with best available resources in the current state of art; i.e. with detector efficiency $\eta_d = 0.88$ and memory efficiency of $\eta_m = 0.87$. And secondly in futurist case where the detectors and memories are more efficient. In that case, similar to the futurist values in previous section, we assume $\eta_m = 0.96$ and $\eta_d = 0.96$. Recent experiments implementing the same protocol [63] have used a pair production probability $p = 0.047$ for the PDC and we assume a repetition rate $\sim 100MHz$ for the PDC source. Assuming outgoing quantum memories with appropriate bandwidth, the comparison results are shown in the two tables below.

We have also assumed a modest repetition rate of $1.5MHz$ for the scheme single photon source. It is obvious if quantum dots are used as single photon sources, the rate R_s in the two tables below will be even higher by an order $\approx 10^3$

Comparison between PDC and Single photon source scheme						
Angle of the polarizer (SPS)/beam splitter (PDC) in degrees	Efficiency		Conditional fidelity		Rate of desired detection	
	E_{sP} (PDC scheme)	E_s (SPS scheme)	f_{sP} (PDC scheme)	f_s (SPS scheme)	R_{sP} (PDC scheme) with a repetition rate $\sim 100\,MHz$	R_s (SPS scheme) with a repetition rate $\sim 1.5\,MHz$
45	63.2%	73.4%	95.5%	95.8%	30	1.4×10^5
60	72.3%	88.6%	92.8%	94.6%	3	6.7×10^4
75	75.8%	95.6%	90.8%	93.8%	0.035	7.6×10^3

Figure 5.5: This table shows theoretically predicted values of efficiency, conditional fidelity, rate of desired detection for different angles of the half wave plate $45^\circ, 60^\circ, 75^\circ$ respectively for the two schemes. Here we have assumed a perfect single photon source with source efficiency $\varepsilon_1 = 0.97$ and $\varepsilon_2 = 0.011$. Current state of art values have been assumed for all other resources such as detector efficiency $\eta_d = 0.88$, memory efficiency $\eta_m = 0.87$. The single photon source is assumed to have a repetition rate of $1.5MHz$. The PDC source is assumed to have a repetition rate of $100MHz$ and probability of production of a perfectly heralded pair $p = 0.047$

Comparison between PDC and Single photon source scheme with $\eta_d = 96\%$, $\eta_m = 96\%$ and $\varepsilon_1 = 99\%$, $\varepsilon_2 = 0.003$						
Angle of the polarizer (SPS)/beam splitter (PDC) in degrees	Efficiency		Conditional fidelity		Rate of desired detection	
	E_{sb} (PDC scheme)	E (SPS scheme)	f_{sb} (PDC scheme)	f (SPS scheme)	R_{sb} (PDC scheme) with a repetition rate $\sim 100\,MHz$	R (SPS scheme) with a repetition rate $\sim 1.5\,MHz$
45	89.3%	88.1%	96%	98.8%	36	1.7×10^5
60	93.7%	94.5%	92.2%	98.4%	5	9.1×10^4
75	95.2%	97.1%	89%	98.1%	0.049	10^4

Figure 5.6: This table shows theoretically predicted values of efficiency, conditional fidelity, rate of desired detection for different angles of the half wave plate $45^\circ, 60^\circ, 75^\circ$ respectively for the two schemes. Here we have assumed a perfect single photon source with source efficiency $\varepsilon_1 = 0.97$ and $\varepsilon_2 = 0.003$. Futurist have been assumed for all other resources such as detector efficiency $\eta_d = 0.96$, memory efficiency $\eta_m = 0.96$. The single photon source is assumed to have a repetition rate of $1.5MHz$. The PDC source is assumed to have a repetition rate of $100MHz$ and probability of production of a perfectly heralded pair $p = 0.047$

5.2.1 Conclusions

In this comparison we have assumed a perfectly heralded PDC source for the PDC scheme and single photon source with near perfect efficiency for the single photon source scheme. The result obtained both in the cases of current state of art and futurist regime points to the fact that for comparable high values of scheme efficiency and conditional fidelity, the rate of desired detection is far too low for the PDC scheme compared to the single photon source scheme even with modest repetition rate for the latter. Thus quantum memories at the output of the PDC scheme needs to have a storage time at least in the order of a few seconds to satisfy the **deterministic criterion** as shown in chapter 3, section 3. Although at the current state of art, the single photon scheme discussed in this thesis can only be implemented with a moderate efficiency of 24% (as shown in chapter 5 section 1.3), it still has a major advantage over the PDC scheme in terms of demand on the storage time of the quantum memories. The demand on storage time for the quantum memory for the scheme using single photon source scheme is smaller than the PDC scheme at least by a factor 10^4 (10^7 if quantum dots are used as single photon source) for comparable high values of scheme efficiency and conditional fidelity, which in turn is necessary for these schemes to work efficiently in the framework of quantum repeaters as mentioned in chapter 2 section 4.2 . Thus we can conclude that if we expect having more efficient resources in the future, successful implementation of a deterministic entangled photon pair sources, with single photon sources will be much more practical than doing the same with the alternate scheme that uses a single PDC source.

Chapter 6

Discussions

We summarize the important conclusions we have obtained in the last two sections.

• A recent repeater architecture [15] has been proposed which uses deterministic entangled photon pair sources. Considering the non multiplexed case, one can think of implementing deterministic entangled photon pair sources using heralded entanglement generating schemes [16] [17] and quantum memories. We have proposed such an implementation using four single photon sources, linear optics, photon number resolving detectors and quantum memories (based on the heralded entanglement generating scheme proposed by Zhang et al [17]). We have assumed the the sources emit *indistinguishable* photons thus the sources emit identical wavepackets.

For optimal performance of the quantum repeater protocol, it is important that the deterministic pair source has high scheme efficiency and high conditional fidelity (chapter 2, section 4.2). The deterministic scheme also demands that the rate of entanglement storage of the scheme must be faster than the inverse of storage time of the quantum memories used (chapter 3, section 3). At the current state of art, it is possible to implement our scheme as a deterministic entangled photon pair source using quantum dots as single photon sources. The predicted conditional fidelity of this scheme at the current state of art is (97%) but the predicted efficiency is moderate at (24%)(chapter 5, section 1.3).

• It is possible to implement single photon source using Parametric Down Conversion source and Quantum Memory with appropriate bandwidth (chapter 2 section 5.2). At the current state of art, where storage time of quantum memories $\sim \mu s$, such implementation is not possible as the rate of creation of deterministic entangled photon pairs does not satisfy the **deterministic criterion** (chapter 3, section 3). For such an implementation, quantum memories of storage time at least $\sim 100\mu s$ is required.

• We can envisage future research where we can think about implementing this scheme as a multiplexed deterministic photon pair source as this would enhance the over all performance of the quantum repeaters.

• Although we have assumed perfect optical components such as half wave plates, polarizing beam splitters, their imperfections will reduce the conditional fidelity by a margin. We look forward to further advancement in their perfection.

• We look forward to further advancement in the fabrication of single photon sources with higher efficiencies and high repetition rate and near perfect indistinguishability. We also look forward to further advancement in fabrication of quantum memories with higher storage time. This advancement will assure implementation of this scheme as a deterministic entangled photon pair source with higher scheme efficiency and conditional fidelity .

• Alternatively it is possible to implement deterministic entangled photon pair sources using linear optics, photon detectors, quantum memories and one parametric down conversion source [16]. But to actually put it into practice, this scheme has a much higher demand of resources than the single photon scheme. So it is fairly conclusive that with the advancements of research, this scheme described in this thesis, which uses single photon sources, has much higher chance of successful implementation than the PDC scheme.

• Future topics of research can be investigating the effect of imperfect indistinguishability of the photons emitted from the four sources. One can also investigate how the repeater protocol discussed in this thesis will perform with this deterministic entangled photon pair source. We have introduced a free parameter θ (see chapter 3, section 1) which can, in principle, be used to optimize the secret key distribution rate of the repeater protocol where this source is implemented (chapter 4, section 4.2).

Bibliography

[1] John S Bell *On the Einstein Podolsky Rosen paradox* Physics, 1, 195 (1964)

[2] R. Horodecki et al *Quantum entanglement* Rev. Mod. Phys. 81, 865 (2009)

[3] A. Einstein et al *Can quantum mechanical description of physical reality can be considered complete?* Phys. Rev. 47, 777 (1935)

[4] A.Aspect et al *Experimental Test of Bell's Inequalities Using Time- Varying Analyzers* PhysRevLett.49,1804 (1982)

[5] A. Aspect et al *Experimental Tests of Realistic Local Theories via Bell's Theorem* PhysRevLett.47,460 (1981)

[6] B. Hensen et al *Loophole-free Bell inequality violation using electron spins separated by 1.3 kilometres* Nature 526, 682 (2015)

[7] Charles H. Bennett, Gilles Brassard, Sandu Popescu, Benjamin Schumacher, John A. Smolin, and William K. Wootters *Purification of Noisy Entanglement and Faithful Teleportation via Noisy Channels* Phys.Rev.Lett.76,722(1996)

[8] Charles H. Bennet, SJ Wiesner *Communication via one- and two-particle operators on Einstein-Podolsky-Rosen states.* Phys. Rev. Lett. 69, 2881 (1992)

[9] A. Ekert *Quantum cryptography based on Bells theorem* Phys. Rev. Lett. 67, 661 (1991)

[10] H. J. Kimble *The Quantum Internet* Nature 453, 1023(2008)

[11] A.S.Holevo *Bounds for the quantity of information transmitted by a quantum communication channel* Probl.Peredachi Inf,9,3,3(1973)

[12] M.Takeoka et al *Fundamental rate-loss tradeoff for optical quantum key distribution* Nature Communications 5, 5235 (2014)

[13] H.J. Briegel, W. Dr, J. I. Cirac, and P. Zoller *Quantum Repeaters: The Role of Imperfect Local Operations in Quantum Communication* Phys. Rev. Lett. 81, 5932(1998)

[14] L.-M. Duan, M. D. Lukin, J. I. Cirac and P. Zoller *Long-distance quantum communication with atomic ensembles and linear optics* Nature 414, 413(2001)

[15] Neil Sinclair et al *Spectral Multiplexing for Scalable Quantum Photonics using an Atomic Frequency Comb Quantum Memory and Feed-Forward Control* Phys. Rev. Lett. 113, 053603 (2014)

[16] C. Sliwa, K. Banaszek *Conditional preparation of maximal polarization entanglement* Phys. Rev. A 67, 030101(R) (2003)

[17] Qiang Zhang et al *Demonstration of a scheme for the generation of event-ready entangled photon pairs from a single-photon source* Phys. Rev. A 77, 062316 (2008)

[18] Nicolas Sangouard, Christoph Simon, Hugues de Riedmatten, and Nicolas Gisin *Quantum repeaters based on atomic ensembles and linear optics* Rev. Mod. Phys, 83, 33 (2011)

[19] C.H.Bennet et al *Teleporting an unknown quantum state via dual classical and Einstein-Podolsky-Rosen channels* Phys. Rev. Lett. 70, 1895 (1993)

[20] C.Simon et al *Quantum Memories A Review based on the European Integrated Project Qubit Applications (QAP)* Eur. Phys. J. D 58, 1 (2010)

[21] Christoph Simon, Hugues de Riedmatten, Mikael Afzelius, Nicolas Sangouard, Hugo Zbinden, Nicolas Gisin *Quantum Repeaters with Photon Pair Sources and Multimode Memories* Phys. Rev. Lett. 98, 190503 (2007)

[22] K.Heshami et al *Quantum memories: emerging applications and recent advances* Journal of Modern Optics 63, S3, S42 (2016)

[23] E.Knill et al *A scheme for efficient quantum computation with linear optics* Nature 409, 46(2001)

[24] L.A.Stewart et al *Single Photon Emission from Diamond nanocrystals in an Opal Photonic Crystal* Opt Express,17(20),18044 (2009)

[25] P.R.Hemmer et al *Raman-excited spin coherences in nitrogen-vacancy color centers in diamond* Optics Letters, 26, 6, 361 (2001)

[26] Charles Santoori et al *Coherent population trapping in diamond N-V centers at zero magnetic field* Optics Express 14, 7986 (2006).

[27] V.M.Acosta et al *Electromagnetically Induced Transparency in a Diamond Spin Ensemble Enables All-Optical Electromagnetic Field Sensing* Phys. Rev. Lett, 110, 213605 (2013)

[28] K.Heshami et al *Raman quantum memory based on an ensemble of nitrogen-vacancy centers coupled to a microcavity* Phys. Rev. A 89, 040301(R) (2014)

[29] E. Poem et al *Broadband noise-free optical quantum memory with neutral nitrogen-vacancy centers in diamond* Phys. Rev. B 91, 205108 (2015)

[30] J.Volz et al *Observation of Entanglement of a Single Photon with a Trapped Atom* Phys. Rev. Lett. 96, 030404 (2006)

[31] K.C.Lee et al *Macroscopic non-classical states and terahertz quantum processing in room-temperature diamond* Nature Photonics 6, 41(2012)

[32] P.J.Bustard et al *Ultrafast slow-light: Raman-induced delay of THz-bandwidth pulses* Phys. Rev. A 93, 043810 (2016)

[33] A.kuzmich et al *Generation of nonclassical photon pairs for scalable quantum communication with atomic ensembles* Nature 423, 731(2003)

[34] M.D.Lukin *Colloquium: Trapping and manipulating photon states in atomic ensembles* Rev. Mod. Phys. 75, 457 (2003)

[35] M.Fleischhauer et al *Quantum memory for photons: Dark-state polaritons* Phys. Rev. A 65, 022314 (2002)

[36] S.A.Moiseev et al *Complete Reconstruction of the Quantum State of a Single-Photon Wave Packet Absorbed by a Doppler-Broadened Transition* Phys. Rev. Lett. 87, 173601 (2001)

[37] B.Kraus et al *Quantum memory for nonstationary light fields based on controlled reversible inhomogeneous broadening* Phys. Rev. A 73, 020302(R) (2006)

[38] A.L.Alexander et al *Photon Echoes Produced by Switching Electric Fields* Phys. Rev. Lett. 96, 043602 (2006)

[39] G.Hetet et al *Electro-Optic Quantum Memory for Light Using Two-Level Atoms* Phys. Rev. Lett. 100, 023601 (2008)

[40] J.J.Longdell et al *Analytic treatment of controlled reversible inhomogeneous broadening quantum memories for light using two-level atoms* Phys. Rev. A 78, 032337 (2008)

[41] B.Lauritzen et al *Telecommunication-Wavelength Solid-State Memory at the Single Photon Level* Phys. Rev. Lett. 104, 080502 (2010)

[42] M.Afzelius et al *Demonstration of Atomic Frequency Comb Memory for light with spin wave storage* Phys. Rev. Lett. 104, 040503 (2010)

[43] M.Sabooni et al *Efficient Quantum Memory Using a Weakly Absorbing Sample* Phys. Rev. Lett. 110, 133604 (2013)

[44] I.Usmani et al *Mapping multiple photonic qubits into and out of one solid-state atomic ensemble* Nature Communications 1: 12 (2010)

[45] M.Bonarota et al *Highly multimode storage in a crystal* New J. Phys. 13, 013013 (2011)

[46] C.Laplane et al *Multiplexed on-demand storage of polarization qubits in a crystal* New J. Phys. 18 013006 (2016)

[47] M.Gundogan et al *Coherent storage of temporally multimode light using a spin-wave atomic frequency comb memory* New J. Phys. 15 045012 (2013)

[48] J.S.Tang et al *Storage of multiple single-photon pulses emitted from a quantum dot in a solid-state quantum memory* Nature Communications 6, 8652 (2015)

[49] E.Saglamyurek et al *Broadband waveguide quantum memory for entangled photons* Nature 469, 512(2011)

[50] S.Guha et al *Rate-loss analysis of an efficient quantum repeater architecture* Phys. Rev. A 92, 022357 (2015)

[51] Z.Q.Zhou et al *Quantum Storage of Three-Dimensional Orbital-Angular-Momentum Entanglement in a Crystal* Phys. Rev. Lett. 115, 070502 (2015)

[52] S.Y.Lan et al *A Multiplexed Quantum Memory* Optics Express ,17, 16, 13639 (2009)

[53] Alain Aspect, Philippe Grangier *Optique quantique 2 : Photons et atomes* Course in Ecole Polytechnique, France

[54] P.W.Shor , J.Preskill *Simple Proof of Security of the BB84 Quantum Key Distribution Protocol* Phys.Rev.Lett.85,441 (2000)

[55] Xing Ding et al *On-Demand Single Photons with High Extraction Efficiency and Near-Unity Indistinguishability from a Resonantly Driven Quantum Dot in a Micro pillar* Phys. Rev. Lett. 116, 020401 (2016)

[56] A.Dousse et al *Ultrabright source of entangled photon pairs* Nature 466, 217 (2010)

[57] Y.Kodriano et al *Radiative cascade from quantum dot metastable spin-blockaded biexciton* Phys. Rev. B 82, 155329 (2010)

[58] M.A.M Versteegh *Observation of strongly entangled photon pairs from a nanowire quantum dot* Nature Communications 5, 5298 (2014)

[59] M.D.Eisaman et al *Single-photon sources and detectors* Rev. Sci. Instrum. 82, 071101 (2011)

[60] Morgan P Hedges et al *Efficient quantum memory for light* Nature 465, 1052(2010)

[61] M. Hosseini *High efficiency coherent optical memory with warm rubidium vapour* Nature Communications 2, 174 (2011)

[62] Dana Rosenberg et al *Noise-free high-efficiency photon-number-resolving detectors* Physical Review A, 71, 061803(R) (2005)

[63] Claudia Wagenknecht et al *Experimental demonstration of a heralded entanglement source* Nature Photonics 4, 549 (2010)

Appendix A

CALCULATIONS

Here we give the expressions of the figures of merit under the imperfections considered showing the calculation steps

A.1 Initial state

A.1.1 Description of the photons

The initial state for the photons emitted from the j^{th} source can be given by

$$\rho_{ij} = (1-\varepsilon_1)\,|0\rangle_{jj}\langle 0| + \varepsilon_1(1-\varepsilon_2)\,|1\rangle_{jj}\langle 1| + \varepsilon_1\varepsilon_2\,|2\rangle_{jj}\langle 2| \forall j = (1,2,3,4) \tag{A.1}$$

Thus the initial joint state of the photons is given by

$$\rho_i = \prod_{\bigotimes j=1}^{4} \rho_{ij} \tag{A.2}$$

In this thesis we approximate that at most one of the sources can emit two photons. With this approximation we can write

$$\rho_{initial} = \lim_{\varepsilon_2^2 \to 0} \rho_i \tag{A.3}$$

With this assumption we note that

$$tr[\rho_{initial}] = 1 \tag{A.4}$$

A.1.2 Pure state calculation

Given a Hilbert space H with finite dimension d, we can write any density matrix in its eigen expansion as

$$\rho = \sum_{i=1}^{d} p_i\,|\phi\rangle_{ii}\langle\phi| \tag{A.5}$$

where $\sum_i p_i = 1$ and $0 \leq p_i \leq 1 \; \forall i$. The vectors $(|\phi_i\rangle)$ forms an orthonormal basis of H

If we define

$$\left|\phi'\right\rangle = \sum_{i}^{d} p_i^{\frac{1}{2}} e^{i\theta_i} \left|\phi\right\rangle_i \tag{A.6}$$

$$\rho' = \left|\phi'\right\rangle \left\langle\phi'\right| \tag{A.7}$$

we can see that ρ is equal to the diagonal elements of ρ'.

A.1.3 Description of the initial state

Following this idea, we can shift our calculation to the pure state formalism. In this way we can write joint pure state of the photons emitted from the j^{th} source

$$\left|\psi\right\rangle_i = \prod_{\otimes j=1}^{4} \left|\psi\right\rangle_j \tag{A.8}$$

where $\left|\psi_j\right\rangle$, which is the initial pure state of any one of the source and is given by

$$\left|\psi\right\rangle_j = [\sqrt{(1-\varepsilon_1)} e^{i\theta'_{0j}} I + \sqrt{\varepsilon_1(1-\varepsilon_2)} e^{i\theta'_{1j}} a_j^\dagger + \sqrt{\frac{\varepsilon_1\varepsilon_2}{2}} e^{i\theta'_{2j}} a_j^{\dagger 2}] \left|0\right\rangle \forall j \subset (1,2,3,4) \tag{A.9}$$

where $a_j^\dagger$ represents the creation operator for each source j and $\theta'_{0j}, \theta'_{1j}, \theta'_{2j}$ are arbitrary phase angles.

From here we can construct $\rho' = \left|\psi\right\rangle_i \left\langle\psi\right|_i$ (equation A.7) and only choose the diagonal elements to retrieve our density matrix ρ_i (equation A.7).

A.2 Circuit

A.2.1 Half Wave Plate

Assuming all the source emit horizontally polarized photons, the half wave plate induce the following transformation on the incoming modes

$a_j^\dagger = \cos\theta a_{jh}^\dagger + \sin\theta a_{jv}^\dagger$ for half wave plates $j = 1,4$

$a_j^\dagger = \sin\theta a_{jh}^\dagger + \cos\theta a_{jv}^\dagger$ for the half wave plates $j = 2,3$.

A.2.2 RPBS

If the detector modes are denoted by $d1h^\dagger$,$d1v^\dagger$,$d2h^\dagger$,$d2v^\dagger$ then the role of *RPBS* is inducing the following mode transformation

$$\begin{pmatrix} a_{1h}^\dagger \\ a_{2v}^\dagger \\ a_{3v}^\dagger \\ a_{4h}^\dagger \end{pmatrix} = \begin{pmatrix} \frac{1}{2} & \frac{1}{2} & \frac{1}{2} & -\frac{1}{2} \\ \frac{1}{2} & \frac{1}{2} & -\frac{1}{2} & \frac{1}{2} \\ \frac{1}{2} & -\frac{1}{2} & \frac{1}{2} & \frac{1}{2} \\ -\frac{1}{2} & \frac{1}{2} & \frac{1}{2} & \frac{1}{2} \end{pmatrix} \begin{pmatrix} d1h^\dagger \\ d1v^\dagger \\ d2h^\dagger \\ d2v^\dagger \end{pmatrix} \tag{A.10}$$

A.2.3 Modelling imperfect detectors

Using the beam splitter model of loss (as shown in Appendix A section 6), the lossy detectors can be modelled as

$$d1h^\dagger = \sqrt{\eta_d} d1h_d^\dagger + \sqrt{1-\eta_m} d1h_l^\dagger \tag{A.11}$$

$$d1v^\dagger = \sqrt{\eta_d} d1v_d^\dagger + \sqrt{1-\eta_m} d1v_l^\dagger \tag{A.12}$$

$$d2h^\dagger = \sqrt{\eta_d} d2h_d^\dagger + \sqrt{1-\eta_m} d2h_l^\dagger \tag{A.13}$$

$$d2v^\dagger = \sqrt{\eta_d} d2v_d^\dagger + \sqrt{1-\eta_m} d2v_l^\dagger \tag{A.14}$$

where modes with subscript d corresponds to cases where the photon has been detected and modes with subscript l corresponds to cases where the photon has not been detected.

A.2.4 Revisiting intial pure state

Now with all the tools in hand, we can re write the initial pure state $|\psi\rangle_i$ (equation A.8) with in the mode expansion involving $(a_{1v}^\dagger, a_{2h}^\dagger, a_{3h}^\dagger, a_{4v}^\dagger, d1h_d^\dagger, d1h_l^\dagger, d1v_d^\dagger, d1v_l^\dagger, d2h_d^\dagger, d2h_l^\dagger, d2v_d^\dagger, d2v_l^\dagger)$
Now we can construct $\rho' = |\psi\rangle_i \langle\psi|_i$ (equation A.7) and only choose the diagonal elements to retrieve our density matrix ρ_i.

A.3 Evaluating figures of merit

A.3.1 Probability of desired joint detection

We have limited ourselves to cases where only one photon emits two photon but we have assumed that this can happen to any source. In our calculation we have checked, that the figures of merit will have the same value for any choice of detector combination $d1h-d2h, d1h-d2v, d1v-d2h, d1v-d2v$.

We choose the detector combination $d1h-d2h$ for the rest of our calculation.

Now, our aim is to evaluate the density matrix of the state after such a desired joint detection ρ_s which we do in the following steps.

We define ρ_2 as follows

$$\rho_2 = tr[\rho_i P_D] \tag{A.15}$$

$$P_D = [d^{\dagger}_{1hd}|0\rangle\langle 0|d_{1hd}] \otimes [d^{\dagger}_{2hd}|0\rangle\langle 0|d_{2hd}] \tag{A.16}$$

ρ_2 is the density matrix after one (and only one) detection in each of the detector pairs $d1h$ and $d2h$. Now we eliminate all terms in ρ_2 which has any of the terms ($d1v$,$d1v^2$,$d1v^3$,$d2v$,$d2v^2$,$d2v^3$). This can be easily done using a computer program. Let us call the remnant density matrix after this elimination ρ_3.

We are still left with the losses that has occurred through any of the detectors. We wish to trace over these losses and it is done as follows. We define

$$P_{d1h_l} = [|0\rangle\langle 0| + d1h_l^{\dagger}|0\rangle\langle 0|d1h_l + \frac{1}{2}d1h_l^{2\dagger}|0\rangle\langle 0|d1h_l^2 + \frac{1}{6}d1h_l^{3\dagger}|0\rangle\langle 0|d1h_l^3] \tag{A.17}$$

$$P_{d1v_l} = [|0\rangle\langle 0| + d1v_l^{\dagger}|0\rangle\langle 0|d1v_l + \frac{1}{2}d1v_l^{2\dagger}|0\rangle\langle 0|d1v_l^2 + \frac{1}{6}d1v_l^{3\dagger}|0\rangle\langle 0|d1v_l^3] \tag{A.18}$$

$$P_{d2h_l} = [|0\rangle\langle 0| + d2h_l^{\dagger}|0\rangle\langle 0|d2h_l + \frac{1}{2}d2h_l^{2\dagger}|0\rangle\langle 0|d2h_l^2 + \frac{1}{6}d2h_l^{3\dagger}|0\rangle\langle 0|d2h_l^3] \tag{A.19}$$

$$P_{d2v_l} = [|0\rangle\langle 0| + d2v_l^{\dagger}|0\rangle\langle 0|d2v_l + \frac{1}{2}d2v_l^{2\dagger}|0\rangle\langle 0|d2v_l^2 + \frac{1}{6}d2v_l^{3\dagger}|0\rangle\langle 0|d2v_l^3] \tag{A.20}$$

With this definition we have

$$\rho_s = tr[tr[tr[tr[\rho_3 P_{d1hm}]P_{d1vm}]P_{d2hm}]P_{d2vm}] \tag{A.21}$$

We can evaluate p_s from in equation 3.4

A.3.2 Scheme efficiency

Modelling imperfect memories

So far we have not considered the memory efficiency as it does not affect the probability of desired joint detection. However the memory efficiency does affect our scheme efficiency. Here we can model the memory efficiency using the beam splitter model of loss. This is exhibited in the following equations

$$a^{\dagger}_{1v} = \sqrt{\eta_m} a^{\dagger}_{1v_{mr}} + \sqrt{1-\eta_m} a^{\dagger}_{1v_{ml}} \tag{A.22}$$

$$a^{\dagger}_{2h} = \sqrt{\eta_m} a^{\dagger}_{2h_{mr}} + \sqrt{1-\eta_m} a^{\dagger}_{2h_{ml}} \tag{A.23}$$

$$a^{\dagger}_{3h} = \sqrt{\eta_m} a^{\dagger}_{3h_{mr}} + \sqrt{1-\eta_m} a^{\dagger}_{3h_{ml}} \tag{A.24}$$

$$a^{\dagger}_{4v} = \sqrt{\eta_m} a^{\dagger}_{4v_{mr}} + \sqrt{1-\eta_m} a^{\dagger}_{4v_{ml}} \tag{A.25}$$

where modes with subscript *mr* corresponds to cases where the outgoing photon has been retrieved from the quantum memory and modes with subscript *ml* corresponds to cases where the outgoing photon in the quantum memory are lost.

We define

$$P_{mr1} = \frac{1}{4}[(a^{\dagger}_{1v_{mr}} + a^{\dagger}_{2h_{mr}}) |0\rangle \langle 0| (a_{1v_{mr}} + a_{2h_{mr}}) + \frac{1}{2}(a^{\dagger}_{1v_{mr}} + a^{\dagger}_{2h_{mr}})^2 |0\rangle \langle 0| (a_{1v_{mr}} + a_{2h_{mr}})^2] \tag{A.26}$$

$$P_{mr2} = \frac{1}{4}[(a^{\dagger}_{4v_{mr}} + a^{\dagger}_{3h_{mr}}) |0\rangle \langle 0| (a_{4v_{mr}} + a_{3h_{mr}}) + \frac{1}{2}(a^{\dagger}_{4v_{mr}} + a^{\dagger}_{3h_{mr}})^2 |0\rangle \langle 0| (a_{4v_{mr}} + a_{3h_{mr}})^2] \tag{A.27}$$

$$P_{mr} = P_{mr1} \otimes P_{mr2} \tag{A.28}$$

This way we can define

$$\rho_{E1} = tr[\rho_s P_{mr}] \tag{A.29}$$

The above step is done to ensure that at least one photon is extracted from each output. Now we again have to trace over the losses incurred due to the inefficiency of the memories. For that, we

again define

$$P_{a_{1v_{ml}}} = [|0\rangle\langle 0| + a^{\dagger}_{1v_{ml}}|0\rangle\langle 0| a_{1v_{ml}} + \frac{1}{2}a^{2\dagger}_{1v_{ml}}|0\rangle\langle 0| a^{2}_{1v_{ml}} + \frac{1}{6}a^{3\dagger}_{1v_{ml}}|0\rangle\langle 0| a^{3}_{1v_{ml}}] \tag{A.30}$$

$$P_{a_{2h_{ml}}} = [|0\rangle\langle 0| + a^{\dagger}_{2h_{ml}}|0\rangle\langle 0| a_{2h_{ml}} + \frac{1}{2}a^{2\dagger}_{2h_{ml}}|0\rangle\langle 0| a^{2}_{2h_{ml}} + \frac{1}{6}a^{3\dagger}_{2h_{ml}}|0\rangle\langle 0| a^{3}_{2h_{ml}}] \tag{A.31}$$

$$P_{a_{3h_{ml}}} = [|0\rangle\langle 0| + a^{\dagger}_{3h_{ml}}|0\rangle\langle 0| a_{3h_{ml}} + \frac{1}{2}a^{2\dagger}_{3h_{ml}}|0\rangle\langle 0| a^{2}_{3h_{ml}} + \frac{1}{6}a^{3\dagger}_{3h_{ml}}|0\rangle\langle 0| a^{3}_{3h_{ml}}] \tag{A.32}$$

$$P_{a_{4v_{ml}}} = [|0\rangle\langle 0| + a^{\dagger}_{4v_{ml}}|0\rangle\langle 0| a_{4v_{ml}} + \frac{1}{2}a^{2\dagger}_{4v_{ml}}|0\rangle\langle 0| a^{2}_{4v_{ml}} + \frac{1}{6}a^{3\dagger}_{4v_{ml}}|0\rangle\langle 0| a^{3}_{4v_{ml}}] \tag{A.33}$$

$$\tag{A.34}$$

Expression for scheme efficiency

Thus

$$\rho_E = tr[tr[tr[tr[\rho_{E1}P_{a_{1v_{ml}}}]P_{a_{2h_{ml}}}]P_{a_{3h_{ml}}}]P_{a_{4v_{ml}}}] \tag{A.35}$$

E_s can be evaluated from equation 3.7

A.3.3 Conditional fidelity

Once we have ρ_E, we can evaluate conditional fidelity from equation 3.8.

A.4 Final expressions

We have

$$\rho_s = \rho_{BS} + \rho_v + \rho_1 + \rho_{211} + \rho_{212} + \rho_{22} + \rho_{31} + \rho_{32} \tag{A.36}$$

where

$$\rho_d = C_{BS}|\Psi\rangle\langle\Psi| \tag{A.37}$$

see equation 3.1. This is the case where the outgoing state is a desired bell state

$$\rho_v = C_v|0\rangle\langle 0| \tag{A.38}$$

This is the case where there is no photon in the output

$$\rho_1 = C_1(|V\rangle_{s1}\langle V_{s1}| + |H_{s2}\rangle\langle H_{s2}| + |H_{s3}\rangle\langle H_{s3}| + |V_{s4}\rangle\langle V_{s4}|) \tag{A.39}$$

This is the case where there is one photon in the output

$$\rho_{211} = C_{211}(|V_{s1}H_{s3}\rangle\langle V_{s1}H_{s3}| + |V_{s1}V_{s4}\rangle\langle V_{s1}V_{s4}| + |H_{s2}H_{s3}\rangle\langle H_{s2}H_{s3}| + |H_{s2}V_{s4}\rangle\langle H_{s2}V_{s4}|) \tag{A.40}$$

$$\rho_{212} = C_{212}(|V_{s1}V_{s4}\rangle\langle V_{s1}V_{s4}| + |H_{s3}H_{s2}\rangle\langle H_{s3}H_{s2}|) \tag{A.41}$$

These are the cases where there is two photons one in each output but they are not in the bell state

$$\rho_{22} = C_{22}(|V_{s1}V_{s1}\rangle\langle V_{s1}V_{s1}| + |V_{s1}H_{s2}\rangle\langle H_{s1}V_{s2}| + |H_{s3}H_{s3}\rangle\langle H_{s3}H_{s3}| + |H_{s2}V_{s4}\rangle\langle H_{s2}V_{s3}|) \tag{A.42}$$

This is the case where there is two photons in the output but they are in the same output mode

$$\begin{aligned}\rho_{31} = C_{31}(&|V_{s4}H_{s3}H_{s2}\rangle\langle V_{s4}H_{s3}H_{s2}| + |V_{s1}H_{s3}H_{s2}\rangle\langle V_{s1}H_{s3}H_{s2}| \\ &+ |V_{s1}V_{s4}H_{s2}\rangle\langle V_{s1}V_{s4}H_{s2}| + |V_{s1}H_{s2}H_{s3}\rangle\langle V_{s1}H_{s2}H_{s3}|)\end{aligned} \tag{A.43}$$

$$\begin{aligned}\rho_{32} = C_{32}(&|V_{s1}V_{s1}V_{s4}\rangle\langle V_{s1}V_{s1}V_{s4}| + |V_{s1}V_{s4}V_{s4}\rangle\langle V_{s1}V_{s4}V_{s4}| \\ &+ |H_{s3}H_{s3}H_{s2}\rangle\langle H_{s3}H_{s3}H_{s2}|) + |H_{s2}H_{s2}H_{s3}\rangle\langle H_{s2}H_{s2}H_{s3}|)\end{aligned} \tag{A.44}$$

These are the cases where there are three photons and at least one in each output mode. The expressions for the coefficients are

$$C_{BS} = \frac{1}{2}(\cos^4\theta)(\sin^4\theta)\varepsilon_1^4(1-4\varepsilon_2)\eta_d^2 \tag{A.45}$$

$$C_v = \frac{1}{2}\eta_d^2(1-\eta_d)^2\varepsilon_1^4(1-4\varepsilon_2)(\cos^8\theta) + (1-\varepsilon_1)^2\varepsilon_1^2(1-2\varepsilon_2)(\cos^4\theta)\eta_d^2 \tag{A.46}$$
$$+4\varepsilon_1^3(1-\varepsilon_1)(1-3\varepsilon_2)\eta_d^2(1-\eta_d)(\cos^6\theta) +$$
$$\varepsilon_2[\frac{1}{2}(1-\varepsilon_1)^3\varepsilon_1(\cos^4\theta)\eta_d^2 + \frac{7}{2}(1-\varepsilon_1)^2\varepsilon_1^2(\cos^6\theta)\eta_d(1-\eta_d)$$
$$+\frac{13}{2}(1-\varepsilon_1)\varepsilon_1^3\eta_d^2(1-\eta_d)^2\cos^8\theta$$
$$+\frac{9}{2}\varepsilon_1^4\eta_d^2(1-\eta_d)^3(\cos^{10}\theta)]$$

$$C_1 = \frac{1}{4}(\cos^6\theta)\sin^2\theta\eta_d^2(1-\eta_d)\varepsilon_1^4(1-4\varepsilon_2) + \frac{1}{4}(1-\varepsilon_1)\varepsilon_1^3(1-3\varepsilon_2)(\cos^4\theta)\sin^2\theta\eta_d^2$$
$$+\varepsilon_2[\frac{7}{8}\varepsilon_1^2(1-\varepsilon_1)^2(\cos^4\theta)\sin^2\theta\eta_d^2 +$$
$$\frac{13}{4}\varepsilon_1^3(1-\varepsilon_1)(\cos^6\theta)\sin^2\theta\eta_d^2(1-\eta_d) + \frac{21}{8}\varepsilon_1^4(\cos^8\theta)\sin^2\theta\eta_d^2(1-\eta_d)^2] \tag{A.47}$$

$$C_{211} = \varepsilon_2[\frac{5}{4}(\cos^4\theta)\sin^4\theta\varepsilon_1^3(1-\varepsilon_1)\eta_d^2 + \frac{5}{4}\varepsilon_1^4(\cos^6\theta)\sin^4\theta\eta_d^2(1-\eta_d)] \tag{A.48}$$

$$C_{212} = \varepsilon_2[\frac{7}{4}(\cos^4\theta)\sin^4\theta\varepsilon_1^3(1-\varepsilon_1)\eta_d^2 + \frac{7}{4}\varepsilon_1^4(\cos^6\theta)\sin^4\theta\eta_d^2(1-\eta_d)] \tag{A.49}$$

$$C_{22} = \varepsilon_2[\frac{1}{4}(\cos^4\theta)\sin^4\theta\varepsilon_1^3(1-\varepsilon_1)\eta_d^2 + \frac{1}{4}\varepsilon_1^4(\cos^6\theta)\sin^4\theta\eta_d^2(1-\eta_d)] \tag{A.50}$$

$$C_{31} = \varepsilon_2[\frac{5}{8}(\cos^4\theta)\sin^6\theta\varepsilon_1^4\eta_d^2] \tag{A.51}$$

$$C_{32} = \varepsilon_2[\frac{1}{4}(\cos^4\theta)\sin^6\theta\varepsilon_1^4\eta_d^2] \tag{A.52}$$

So we have

$$p_s = 4(C_{BS} + C_v + 2C_{212} + 4(C_1 + C_{211} + C_{22} + C_{31} + C_{32})) \tag{A.53}$$

Again

$$\rho_E = \rho_{E1} + \rho_{E2} \tag{A.54}$$

where

$$\begin{aligned}\rho_{E1} = \eta_m^2 C_{BS} \left|BS\right\rangle \left\langle BS\right| \\ +\eta_m^2 C_{211}(\left|V_{s1}H_{s2}\right\rangle \left\langle V_{s1}H_{s2}\right| + \left|V_{s4}H_{s3}\right\rangle \left\langle V_{s4}H_{s3}\right| + \\ +\eta_m^2 C_{212}(\left|V_{s1}V_{s4}\right\rangle \left\langle V_{s1}V_{s4}\right| + \left|H_{s3}H_{s2}\right\rangle \left\langle H_{s3}H_{s2}\right|)\end{aligned} \tag{A.55}$$

and

$$\begin{aligned}\rho_{E2} = \eta_m^3 C_{31}(\left|V_{s4}H_{s3}H_{s2}\right\rangle \left\langle V_{s4}H_{s3}H_{s2}\right| \\ + \left|V_{s1}H_{s3}H_{s2}\right\rangle \left\langle V_{s1}H_{s3}H_{s2}\right| \\ + \left|V_{s1}V_{s4}H_{s2}\right\rangle \left\langle V_{s1}V_{s4}H_{s2}\right| \\ + \left|V_{s1}a_{2h}H_{s3}\right\rangle \left\langle V_{s1}a_{2h}H_{s3}\right|) \\ +\eta_m^3 C_{32}(\left|V_{s1}V_{s1}V_{s4}\right\rangle \left\langle V_{s1}V_{s1}V_{s4}\right| \\ + \left|V_{s1}V_{s4}V_{s4}\right\rangle \left\langle V_{s1}V_{s4}V_{s4}\right| \\ + \left|H_{s3}H_{s3}H_{s2}\right\rangle \left\langle H_{s3}H_{s3}H_{s2}\right| \\ + \left|H_{s2}H_{s2}H_{s3}\right\rangle \left\langle H_{s2}H_{s2}H_{s3}\right|)\end{aligned} \tag{A.56}$$

and

$$\rho_{bellstate} = \rho_d = C_{BS} \left|\Psi\right\rangle \left\langle \Psi\right| \tag{A.57}$$

So we have (from equation 3.7 and equation 3.8)

$$E_s = \frac{4\eta_m^2(C_{BS} + 2(C_{211} + C_{212}) + 4\eta_m(C_{31} + C_{32}))}{p_s} \tag{A.58}$$

$$f_s = \frac{1}{1 + \varepsilon_2 \frac{f1}{f2}} \tag{A.59}$$

where

$$f1 = \frac{1}{\varepsilon_2}(2(C_{211}+C_{212})+4\eta_m(C_{31}+C_{32}) \tag{A.60}$$

$$f2 = C_{BS} \tag{A.61}$$

We can see that for small values of ε_2 we can write

$$f_s = 1-\varepsilon_2\frac{f1}{f2} \tag{A.62}$$

A.5 Additional- an interesting property of the RPBS

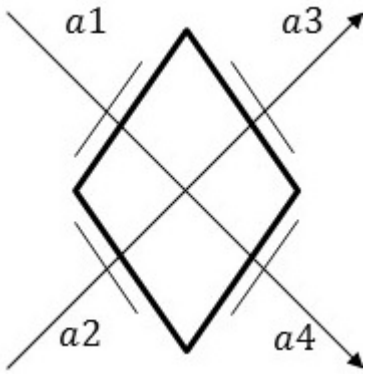

Figure A.1: Schematic diagram of a rotated polarizing beam splitter. A rotated polarizing beam splitter is an ordinary polarizing beam splitter with half wave plates with an angle $\pi/4$ at each of its entry and exit. The annihilator operator of the incoming modes are denoted as $a1$ and $a2$ while the annihilator outgoing modes are denoted as $a3$ and $a4$

Here we consider a few properties of the *RPBS* where two photons are entering and emerging from it.

A.5.1 Two photons from same input

First we ask the question what happens if we we have two photons incoming from one end and none from the other? In the case we can write the incoming state as $\frac{1}{2}(\alpha_1 a1_h^\dagger + \beta_1 a1_v^\dagger)^2 + (\alpha_2 a2_h^\dagger + \beta_2 a2_v^\dagger)^2 |0\rangle$ and expanding it after the mode transformation, as described above, we have the final state in the linear combinations of the terms $(a3_h^{2\dagger}, a3_v^{2\dagger}, a4_h^{2\dagger}, a4_v^{2\dagger}, a3_h^\dagger a3_v^\dagger, a4_h^\dagger a4_v^\dagger)$ acting on $|0\rangle$. As we can see that each of the terms are either in $a3^\dagger$ OR in $a4^\dagger$, but there are no terms which are in product of $a3^\dagger$ and $a4^\dagger$, we can say that if we have two incoming photons from the same input in the *RPBS*, then they will emerge at the same output of *RPBS*.

A.5.2 Two photons from different input

If they arrive at different output, then we can write the incoming state as $(\alpha_1 a1_h^\dagger + \beta_1 a1_v^\dagger)(\alpha_2 a2_h^\dagger + \beta_2 a2_v^\dagger) |0\rangle$ and and expanding it after the mode transformation, as described above, we have the final state in the linear combinations of the terms $(a3_h^{2\dagger}, a3_v^{2\dagger}, a4_h^{2\dagger}, a4_v^{2\dagger}, a3_h^\dagger a4_h^\dagger, a3_h^\dagger a4_v^\dagger, a3_v^\dagger a4_h^\dagger, a3_v^\dagger a4_v^\dagger)$ acting on $|0\rangle$. This clears the fact that if we have two photons emerging from different outputs in the *RPBS*, i.e. the outgoing terms are in product form of the modes $a3^\dagger$ and $a4^\dagger$, then they must have entered the *RPBS* from different inputs.

A.5.3 Polarization parity and RPBS

Here we stick to the case where two photons are incoming on the *RPBS* from two different input. A photon in each of these mode can either be horizontally polarized or vertically polarized. Thus the *RPBS* matrix performs the following transformation

$$\begin{pmatrix} |H\rangle_{a3}|H\rangle_{a4} \\ |H\rangle_{a3}|V\rangle_{a4} \\ |V\rangle_{a3}|H\rangle_{a4} \\ |V\rangle_{a3}|V\rangle_{a4} \end{pmatrix} = \begin{pmatrix} \frac{1}{2} & \frac{1}{2} & \frac{1}{2} & -\frac{1}{2} \\ \frac{1}{2} & \frac{1}{2} & -\frac{1}{2} & \frac{1}{2} \\ \frac{1}{2} & -\frac{1}{2} & \frac{1}{2} & \frac{1}{2} \\ -\frac{1}{2} & \frac{1}{2} & \frac{1}{2} & \frac{1}{2} \end{pmatrix} \begin{pmatrix} |H\rangle_{a1}|H\rangle_{a2} \\ |H\rangle_{a1}|V\rangle_{a2} \\ |V\rangle_{a1}|H\rangle_{a2} \\ |V\rangle_{a1}|V\rangle_{a2} \end{pmatrix} \tag{A.63}$$

Thus if the incoming state has same polarization, either both horizontally polarized or both vertically polarized with the same probability, i.e. if the initial (un-normalized) vector is $(1,0,0,1)^T$ then the *RPBS* transforms it into the outgoing vector $(0,1,1,0)^T$ which implies that the outgoing state has opposite polarization.

Similarly if the incoming state has opposite polarization, either both horizontally polarized or both vertically polarized with the same probability, i.e. if the initial (un-normalized) vector is $(0,1,1,0)^T$ then the *RPBS* transforms it into the outgoing state $(1,0,0,1)^T$ which implies that the outgoing state has same polarization.

A.6 Additional - beam splitter model of loss

An optical element, such as a detector or a quantum memory with an efficiency η can be modelled using a perfect element and a beam splitter with a transitivity $\sqrt{\eta}$ placed in front of it.

$$a_{in} = \sqrt{\eta} a^{\dagger}_{eff} + \sqrt{1-\eta} a^{\dagger}_{loss} \tag{A.64}$$

If a photon is transmitted through this beam splitter, it is equivalent to the scenario where the optical element functions efficiently (denoted by subscript eff) and the if the photon is reflected through this beam splitter, it is equivalent to the scenario where the optical element fails to function, (denoted by subscript *loss*).

A.7 Additional - Entanglement swapping

Entanglement swapping [19] is a measurement technique to create entanglement between two subsystems which have not interacted previously. If the joint system A,B and C,D are previously entangled, the idea behind entanglement swapping is to interfere subsystems B and C to create entanglement between subsystems A and D who have not previously entangled. Quantum repeaters rely on entanglement swapping either by one photon or two photon detections as described below.

Via one photon detection

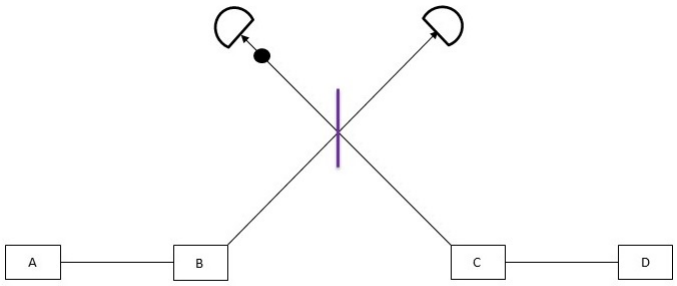

Figure A.2: Schematic diagram of entanglement swapping via one photon detection

Let us assume that subsystems A and B are optically entangled via de-localization of a single photon among them. We can write

$$|\Psi\rangle_{AB} = \frac{1}{\sqrt{2}}(a_A^\dagger + a_B^\dagger)\,|0\rangle \tag{A.65}$$

Similarly subsystems C and D are optically entangled via de-localization of a single photon among them. We can write

$$|\Psi\rangle_{CD} = \frac{1}{\sqrt{2}}(a_C^\dagger + a_D^\dagger)\,|0\rangle \tag{A.66}$$

Thus their joint subsystem can be written as

$$|\Psi\rangle = |\Psi\rangle_{AB} \otimes |\Psi\rangle_{CD} \tag{A.67}$$

If photons from B and C are allowed to be incident on the beam splitter (figure A.2), then denoting the beam splitter output modes as $a_E^\dagger$ and $a_F^\dagger$, the joint system can be written as

$$|\Psi\rangle = \frac{1}{2}[\frac{1}{2}a_E^{2\dagger} - \frac{1}{2}a_F^{2\dagger} + a_A^\dagger a_D^\dagger + a_E^\dagger \frac{1}{\sqrt{2}}(a_A^\dagger + a_D^\dagger) - a_F^\dagger \frac{1}{\sqrt{2}}(a_A^\dagger - a_D^\dagger)]\,|0\rangle \tag{A.68}$$

The last two terms corresponds to the case where a single photon is detected either along the detector in the mode $a_E^\dagger$ or in the mode $a_F^\dagger$ and subsystems A and D are subsequently entangled and this happens with a 50% probability. Single photon entanglement swapping is employed in quantum repeater protocols such as the DLCZ protocol [14]

Via two photon detection

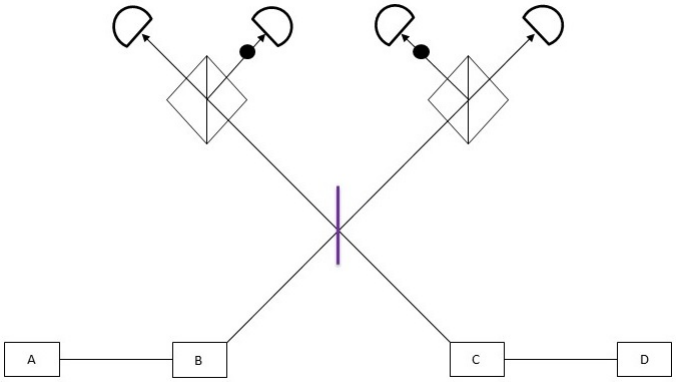

Figure A.3: Schematic diagram of entanglement swapping via two photon joint detections

In this case let us assume that two photons, one in each subsystems A and B, are entangled in their polarization mode. We can write

$$|\Psi\rangle_{AB} = \frac{1}{\sqrt{2}}(a^{\dagger}_{AH}a^{\dagger}_{BH} + a^{\dagger}_{AV}a^{\dagger}_{BV})\,|0\rangle \tag{A.69}$$

Similarly subsystems C and D, are entangled in their polarization mode. We can write

$$|\Psi\rangle_{CD} = \frac{1}{\sqrt{2}}(a^{\dagger}_{CH}a^{\dagger}_{DH} + a^{\dagger}_{CV}a^{\dagger}_{DV})\,|0\rangle \tag{A.70}$$

Thus their joint subsystem can be written as

$$|\Psi\rangle = |\Psi\rangle_{AB} \otimes |\Psi\rangle_{CD} \tag{A.71}$$

If photons from B and C are allowed to be incident on the beam splitter followed by two polarizing beam splitters, one in each outgoing mode (figure A.3), then denoting the polarizing beam splitter

output modes as ($a^{\dagger}_{EH}$,$a^{\dagger}_{EV}$) and ($a^{\dagger}_{FH}$,$a^{\dagger}_{FV}$), the joint system can be written as

$$\begin{aligned}
|\Psi\rangle = \frac{1}{2}[&\frac{1}{2}a^{2\dagger}_{EH}a^{\dagger}_{AH}a^{\dagger}_{DH} \\
&-\frac{1}{2}a^{2\dagger}_{FH}a^{\dagger}_{AH}a^{\dagger}_{DH} \\
&+\frac{1}{2}a^{2\dagger}_{EV}a^{\dagger}_{AV}a^{\dagger}_{DV} \\
&-\frac{1}{2}a^{2\dagger}_{FV}a^{\dagger}_{AV}a^{\dagger}_{DV} \\
&+\frac{1}{\sqrt{2}}a^{\dagger}_{EH}a^{\dagger}_{EV}\frac{1}{\sqrt{2}}(a^{\dagger}_{AH}a^{\dagger}_{DV}+a^{\dagger}_{AV}a^{\dagger}_{DH}) \\
&-\frac{1}{\sqrt{2}}a^{\dagger}_{FH}a^{\dagger}_{FV}\frac{1}{\sqrt{2}}(a^{\dagger}_{AH}a^{\dagger}_{DV}+a^{\dagger}_{AV}a^{\dagger}_{DH}) \\
&+\frac{1}{\sqrt{2}}a^{\dagger}_{EV}a^{\dagger}_{FH}\frac{1}{\sqrt{2}}(a^{\dagger}_{AH}a^{\dagger}_{DV}-a^{\dagger}_{AV}a^{\dagger}_{DH}) \\
&-\frac{1}{\sqrt{2}}a^{\dagger}_{EV}a^{\dagger}_{FH}\frac{1}{\sqrt{2}}(a^{\dagger}_{AH}a^{\dagger}_{DV}-a^{\dagger}_{AV}a^{\dagger}_{DH})]\,|0\rangle
\end{aligned} \tag{A.72}$$

The last four terms corresponds to the case where two photons are detected, one in each detectors. One can see that such a joint detection creates entanglement between subsystems A and D with a probability of 50%. Entanglement swapping via two photon detection is used in the quantum repeater protocol discussed in this thesis [15].

Appendix B

Scheme using parametric down conversion source

In this chapter we outline an alternate scheme where deterministic entangled photon pairs can be generated using parametric down conversion source and give expressions of the figures of merit

B.1 Description

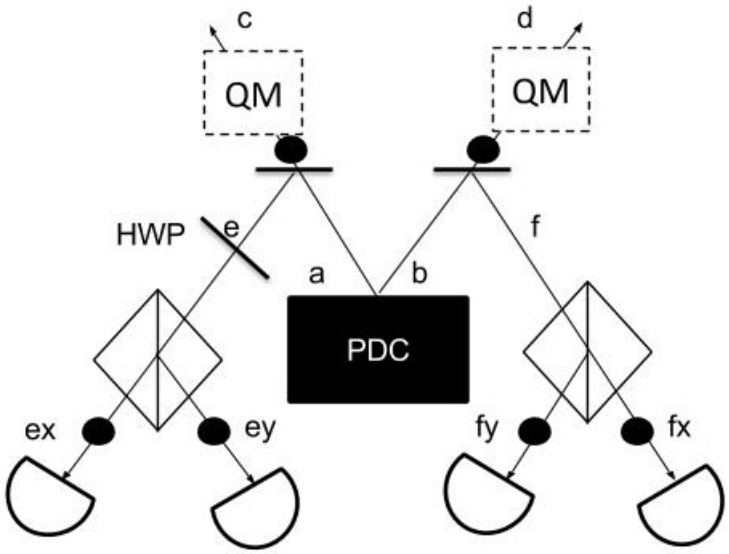

Figure B.1: Deterministic entangled photon pair source using parametric down conversion source

This alternative approach is based on the heralded entanglement scheme proposed by Sliwa and Banaszek [16]. A parametric down conversion source emits three polarization entangled photon pairs in the mode a and b. Each mode is incident on a beam splitter where each photon can be transmitted and subsequently stored in quantum memories marked QM. Or they can be reflected back to a polarizing beam splitter whose output modes lead to a pair of photon number resolving detectors. A half wave plate is placed before the polarizing beam splitter of any of the one mode,

here along mode e. A fourfold detection, one in each four detectors, heralds storage of a pair of polarization entangled photons in the output mode.

It is trivial from the scheme that if the PDC source emits one pair of photon, it cannot lead to a fourfold detection. If it emits two pair of photons, and if all of them are reflected from the respective beam splitters along modes e and f, the presence of the half wave plate in mode e ensures that the two photons along e are both directed to any one of the detectors due to the Hong Ou Mandel effect. Thus such a four fold detection is not possible. In the ideal case, if the PDC source emits three pairs of photons, then the fourfold detection ensures storage of one photon in each of the output modes c and d. As the stored photons can have any of the two orthogonal polarizations with equal probability, they are in a bell state.

The notions of probability of fourfold detection p_{sP}, rate of joint detection R_{sP} scheme efficiency E_{sP} and conditional fidelity f_{sP} can similarly defined in this case.

B.2 Imperfections

Imperfection in this scheme can arise from non unit detector efficiency η_d, memory efficiency η_m, and emission of four pairs of photons instead of three pairs. Another source of error is the non unit heralding efficiency of the PDC source. Although in this thesis, we have considered a perfectly heralded PDC source. If the probability of emission of one photon pair in a spontaneous parametric down conversion is p then probability of three photon pair emission is proportional to p^3 and the probability of four pair emission is proportional to p^4. Here one can note that the success probability (p^3) and the probability of multiple emissions (p^4) cannot be treated independently, unlike the case in the scheme described in this thesis.

B.3 Figures of merit

Assuming a perfectly heralded PDC source which can emit a pair of polarization entangled pair of photons with a probability p, and photon number detectors with detector efficiency η_d, memory efficiency η_m and reflectivity of each of the beam splitters as $\sin\theta$ we give the expressions for probability of desired detection p_{sP},conditional fidelity f_{sP}, scheme efficiency E_{sP}.

If we consider emission upto four pair of photons, the trace of the input state is given by

$$tr[\rho_{inputP}] = 1 + p + \frac{3}{4}p^2 + \frac{1}{2}p^3 + \frac{5}{16}p^4 \tag{B.1}$$

As the probability of emission of a pair from a PDC $\sim 10^{-2}$, we can approximate $tr[\rho_{inputP}] \approx 1$. With this approximation, the probability of desired detection p_{sP} is given by

$$p_{sP} = \frac{p^3}{4}\eta_d^4 \sin^8\theta(1-\eta_d\sin^2\theta)^2(1+\frac{13}{4}p(1-\eta_d\sin^2\theta)^2) \tag{B.2}$$

Thus

$$R_{sP} = p_{sP} \times R_{rep} \tag{B.3}$$

where R_{rep} is the repetition rate of the PDC which is taken to be $\sim 100MHz$ The scheme efficiency for the PDC scheme E_{sP}

$$E_{sP} = \frac{\eta_m^2\cos^4\theta}{(1-\eta_d\sin^2\theta)^2}\frac{(1+p\frac{13}{8}\eta_d^4\sin^8\theta(\eta_m^2\cos^4\theta+4\eta_m(1-\eta_d)\cos^2\theta\sin^2\theta+4(1-\eta_d)^2\sin^4\theta)}{1+\frac{13}{4}p(1-\eta_d\sin^2\theta)^2} \tag{B.4}$$

The conditional fidelity f_{sP} is given by

$$f_{sP} = \frac{1}{1+13p(\frac{1}{4}\cos^4\theta\eta_m^2+(1-\eta_d)\cos^2\theta\sin^2\theta\eta_m+(1-\eta_d)^2\sin^4\theta)} \tag{B.5}$$

B.4 Additional - PDC

The wave function of a perfectly heralded parametric down conversion source emitting n pairs of polarization entangled photons along modes a and b with orthogonal polarization directions x and

y can be described as

$$|\psi\rangle = \sum_{n=0}^{\infty} \lambda_n |\psi_n\rangle \tag{B.6}$$

where

$$\lambda_n = \sqrt{n+1}\frac{\tanh^n r}{\cosh^n r} \tag{B.7}$$

the probability amplitude of generating n photon pairs. Here r is a dimensionless parameter proportional to the interaction time. And $|\psi_n\rangle$ is the normalised n pair component wave function given by

$$|\psi_n\rangle = \frac{1}{n!\sqrt{n+1}}(a_x^\dagger b_y^\dagger - a_y^\dagger b_y^\dagger)^n |0\rangle \tag{B.8}$$